



Elettra Sincrotrone Trieste



Elettra
Sincrotrone
Trieste

Infrared spectroscopies with synchrotron radiation and free electron lasers

Part II

THz studies with Storage Rings and Free Electron Laser radiation



Outline

The THz spectral range

THz spectroscopy with Synchrotron Radiation

Accelerator-based Coherent sources of THz light

TeraFERMI – the THz beamline at FERMI

THz studies with FELs



Outline

The THz spectral range

THz spectroscopy with Synchrotron Radiation

Accelerator-based Coherent sources of THz light

TeraFERMI – the THz beamline at FERMI

THz studies with FELs

The Terahertz Gap

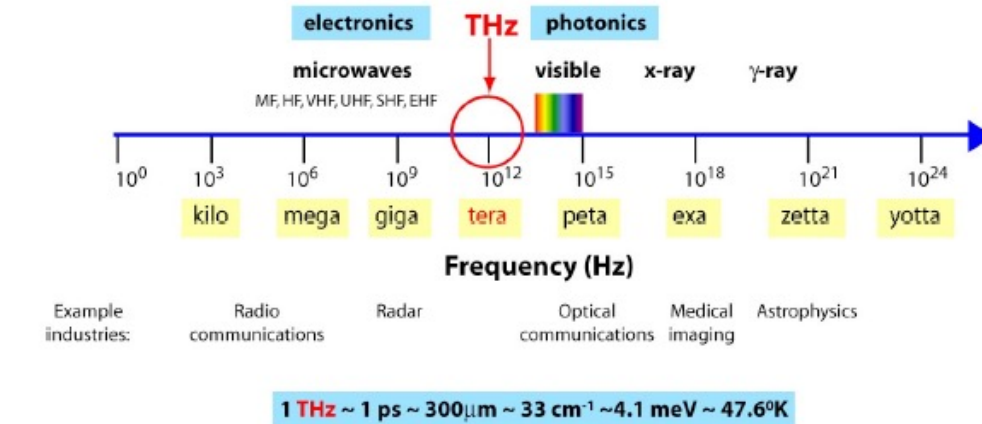
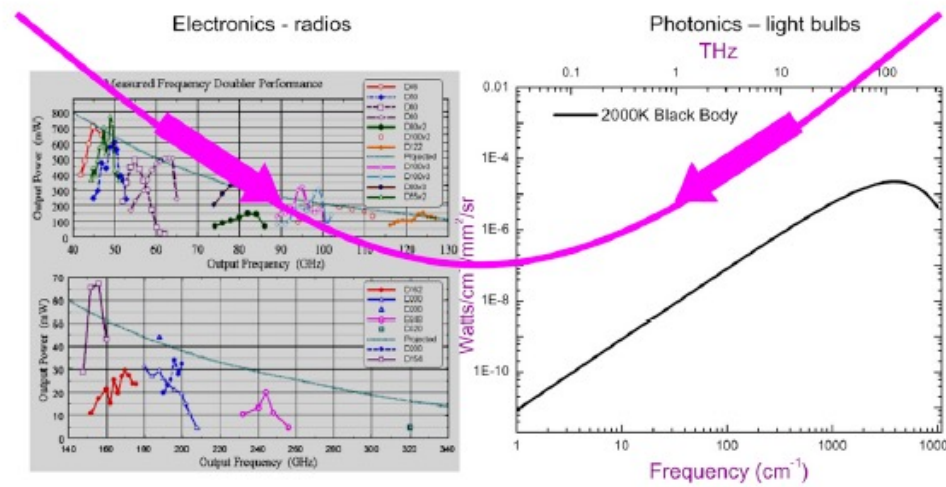


Figure 1. Schematic of the electromagnetic spectrum showing that THz light lies between electronics and photonics.



G. Williams, Rep Prog Phys (2006)



Properties of THz light

- **Non-ionizing**

safe use on living people/animals, non-destructive for biological samples

- **Highly penetrating**

sees through many materials, as packaging, clothing, walls

- **Chemical specificity**

distinguishes between different plastics, drugs, explosives

- **High contrast**

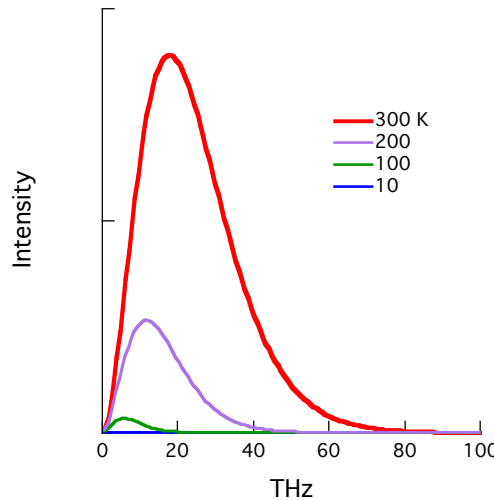
between strong (metals, water) and weak (plastics, tissues) absorbers

- **High-speed communications**

1000 times faster than GHz

...the main drawback is spatial resolution ~ mm

THz light and blackbody radiation



Planck's law

$$I(\nu, T) = \frac{2h\nu^3}{c^2} \frac{1}{e^{\frac{h\nu}{kT}} - 1}$$

Wien's law

$$\begin{aligned}\lambda_{\max} &= b/T & b &= 2.897 \cdot 10^{-3} \text{ K m} \\ \nu_{\max} &= 0.1035 T & \text{THz K}^{-1}\end{aligned}$$

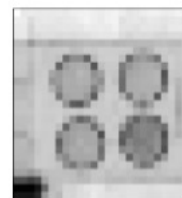
→ All objects at room temperature are THz radiation emitters



→ THz modes are normally populated at room T

Technological applications

Pharmaceutical



Chemical recognition

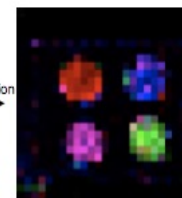
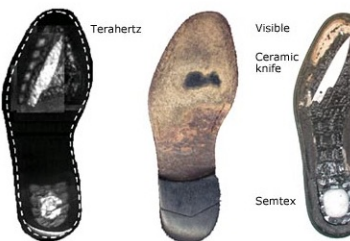


Fig. 8. Visible image of sample with four pellets containing different chemicals: (1) lactose, (2) aspirin, (3) sucrose, and (4) tartaric acid.

Security



Quality control

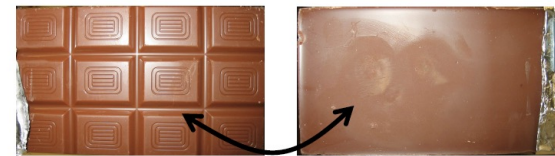
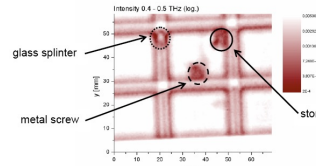


Figure 3. Front and back side of a chocolate bar after artificial contamination with a stone, a M2 metal screw and a glass splinter.



Medical imaging

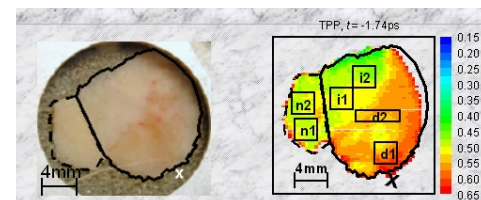


Table-top THz sources

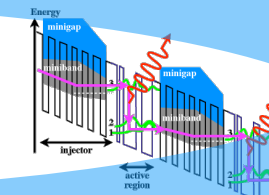
Monochromatic Sources

Backward-Wave-Oscillators



Gas Lasers (CO₂ and CO₂-pumped)
Si/Ge Lasers

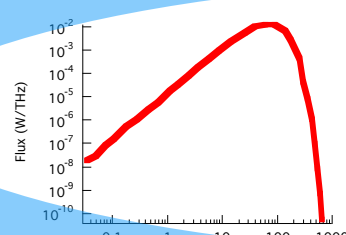
Quantum Cascade Lasers



Broadband Sources

Globar (blackbody source)

silicon carbide rod electrically heated up to 1000 to 1650°C



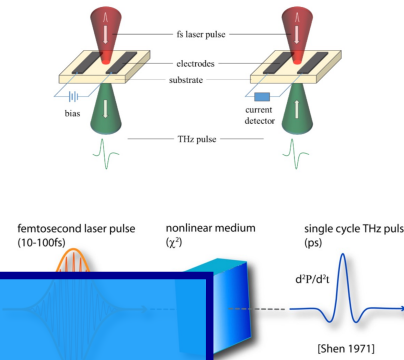
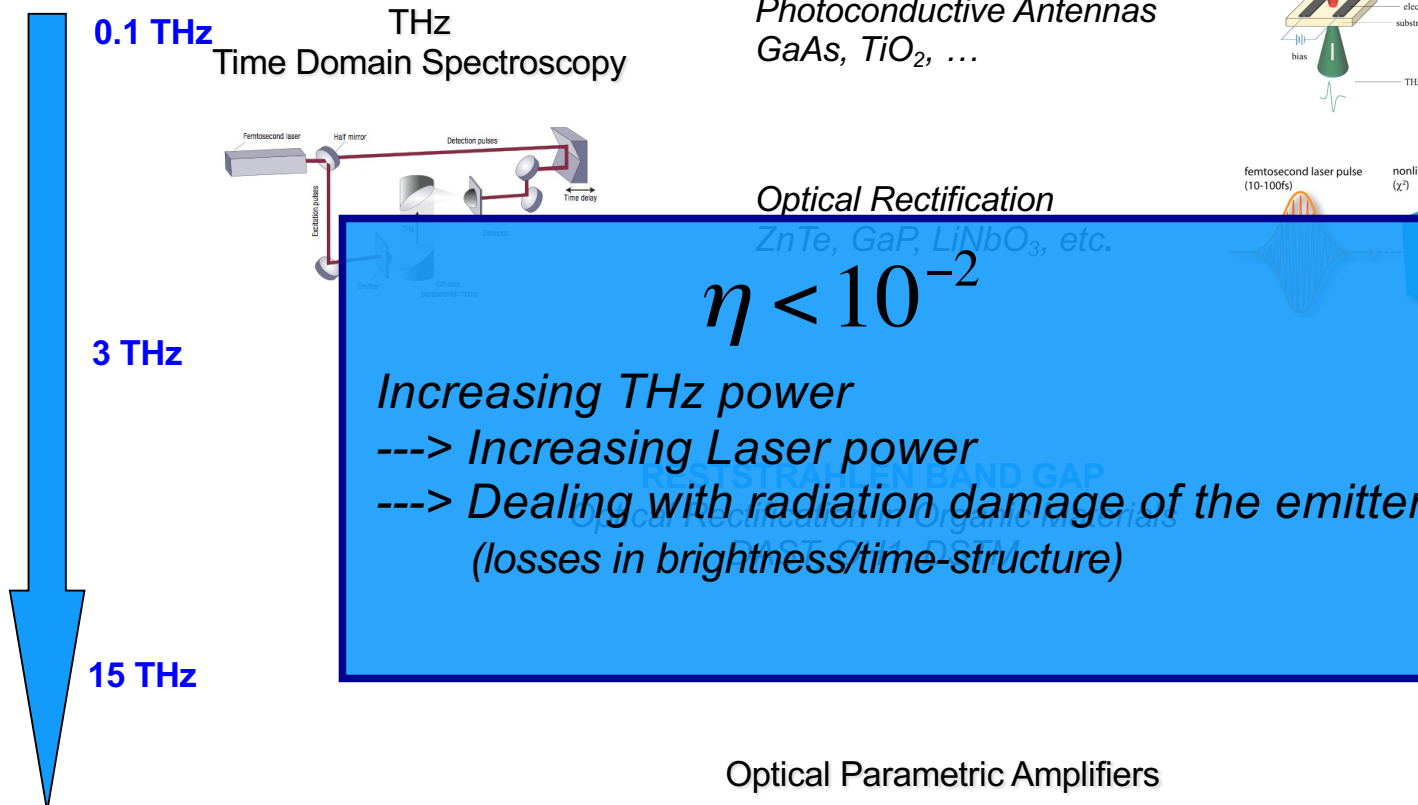
Total Flux:
10 µW between 0-1 THz
5 mW between 0-10 THz
1,5 W between 0-100 THz

Because of poor collimation
typically one has nW power at
sample at THz frequencies

Hg-lamp
Performs slightly better than Globar, below 5 THz



Femtosecond THz sources

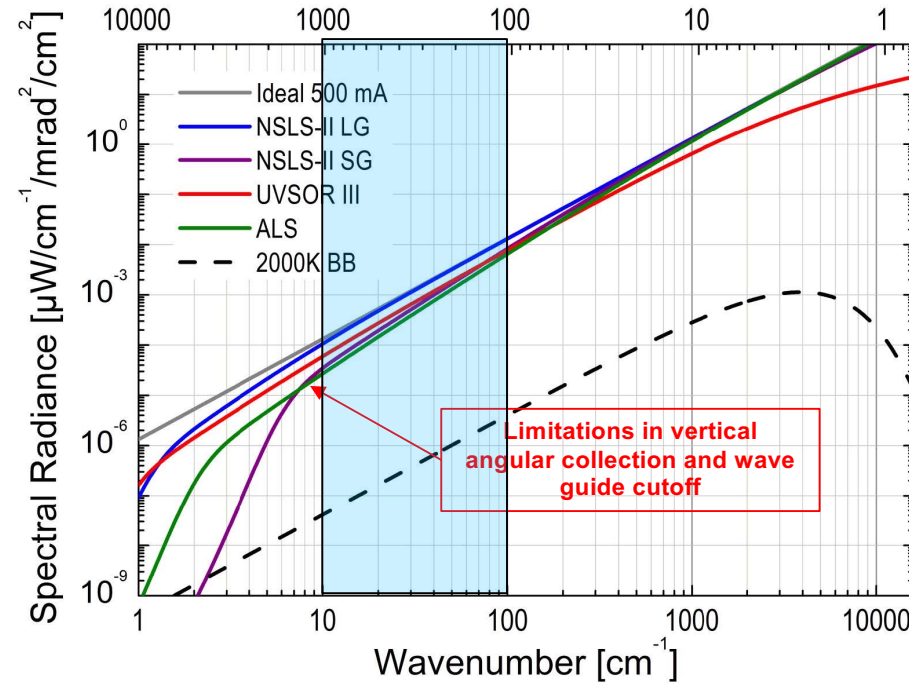
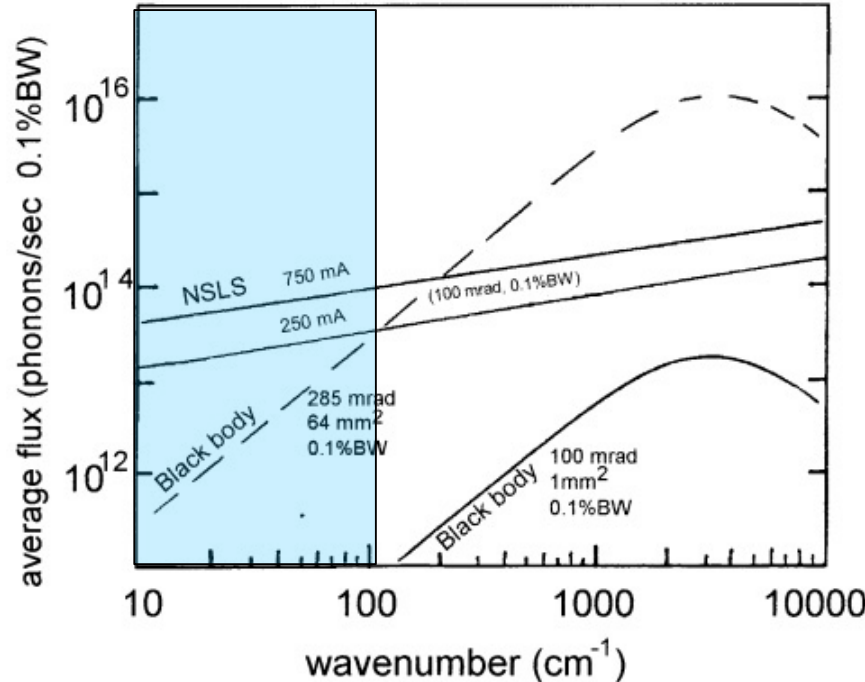


Optical Parametric Amplifiers
Tunable, Narrow-Band



Elettra
Sincrotrone
Trieste

IRSR – The spectral radiance advantage



P. Dumas, M.C. Martin, G.L. Carr 2020



Outline

The THz spectral range

THz spectroscopy with Synchrotron Radiation

Accelerator-based Coherent sources of THz light

TeraFERMI – the THz beamline at FERMI

THz studies with FELs



Elettra
Sincrotrone
Trieste

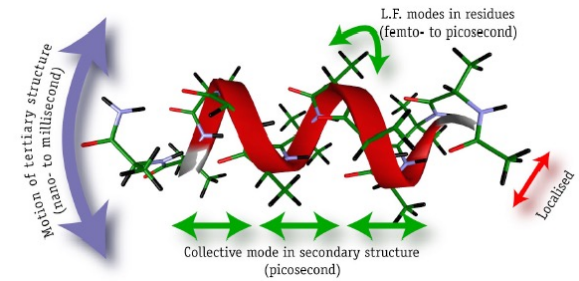
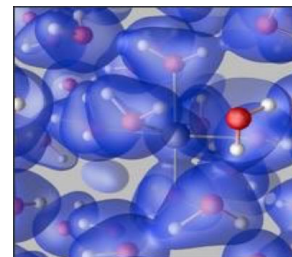
THz Spectroscopy

Superconductivity
Collective excitations
Multiferroics
Heterostructures
Metamaterials
Plasmonics

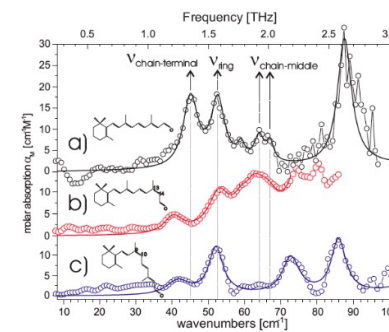


Graphene
2D chalcogenides
Black Phosphorus

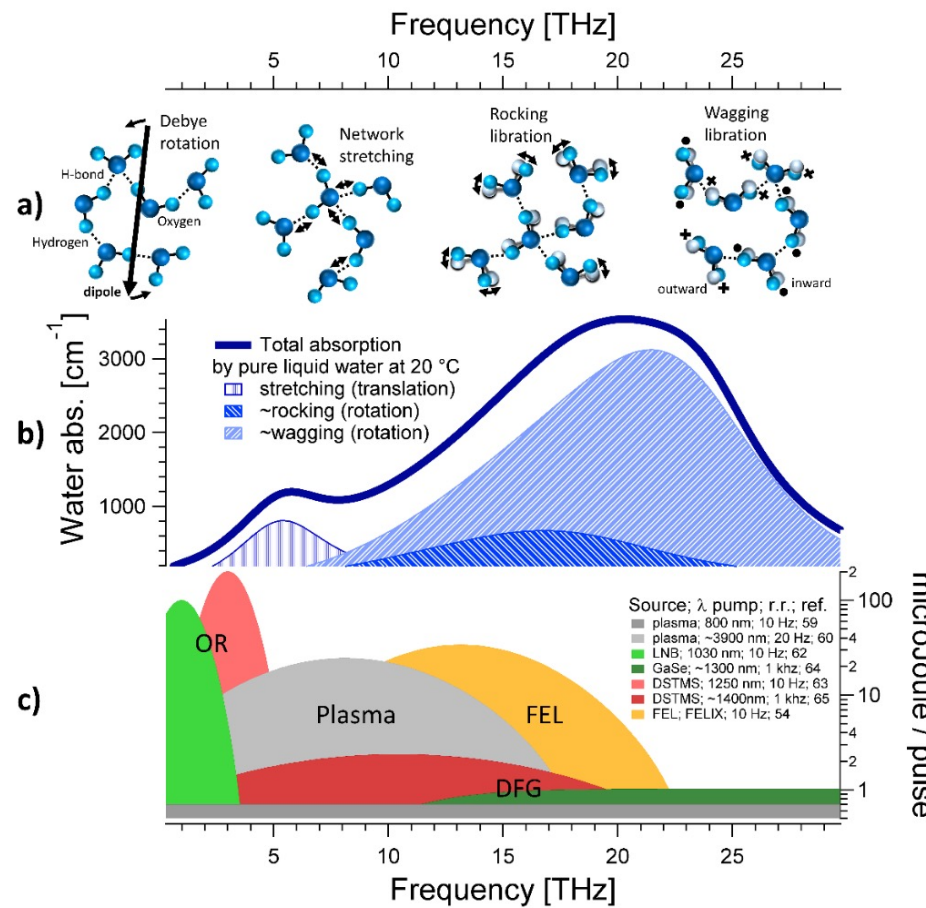
Polar liquids
Hydrogen bonds
Van der Waals interactions
Solutions



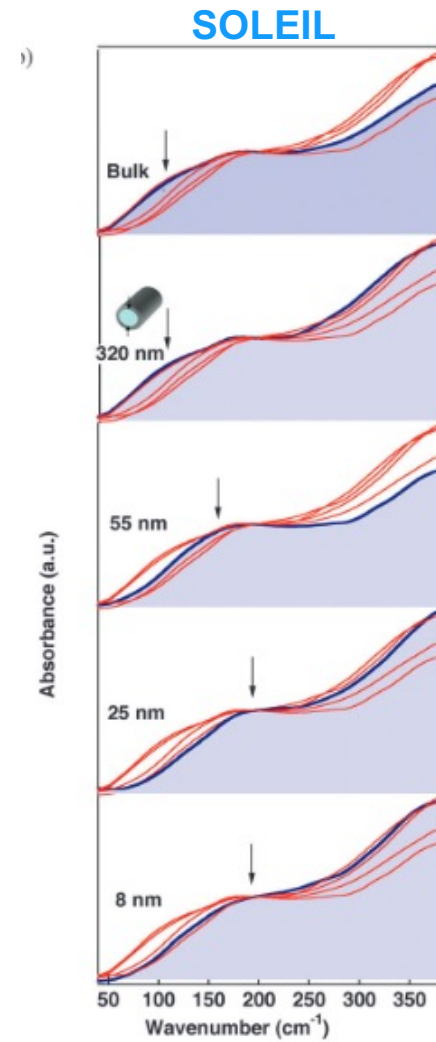
Protein Folding
Amyloid fibrils
Isomers



THz modes in water



F. Novelli et al., Materials 2020

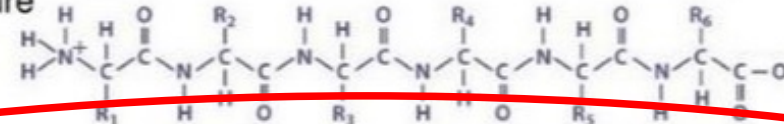


S. Le Caer et al., Phys Chem Chem Phys 2011

Hyerarchical structure of proteins

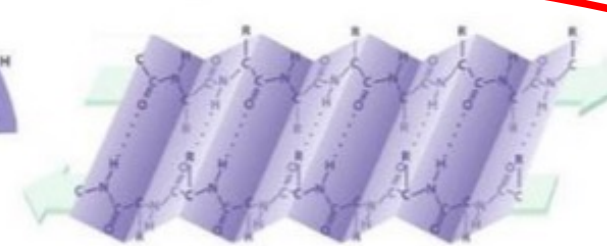
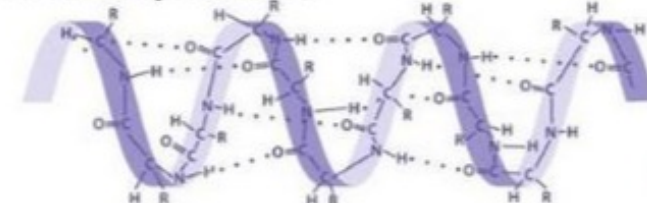
a)

primary structure



b)

secondary structure



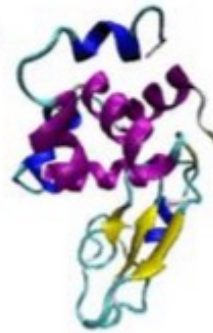
IR

α helix

β sheet

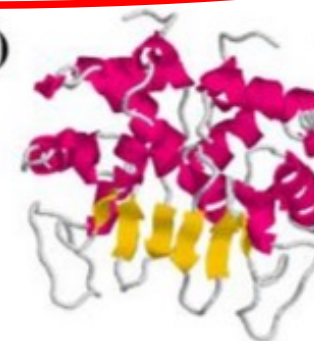
c)

tertiary structure



d)

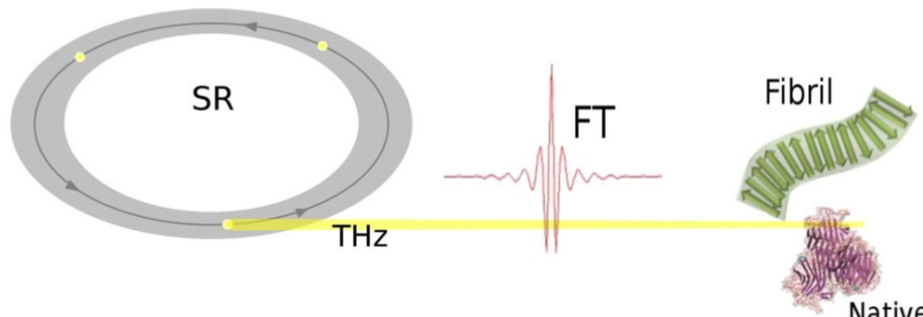
quaternary structure



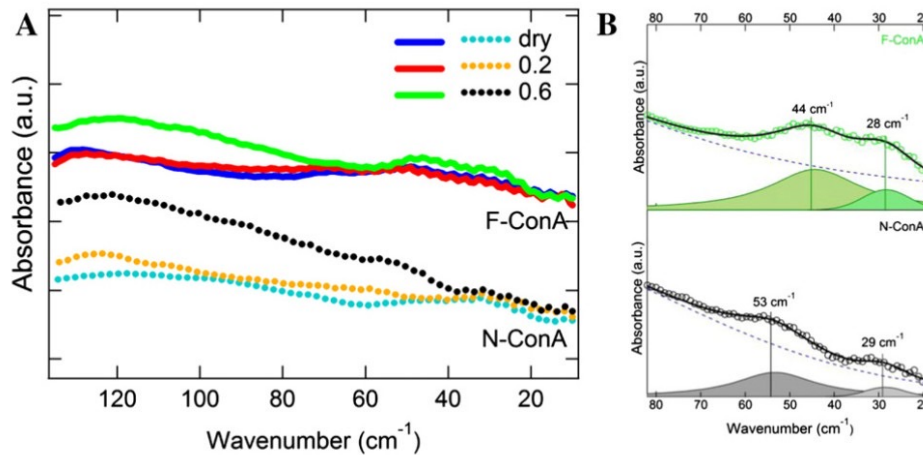
THz

(Martin A Schroer 2011)

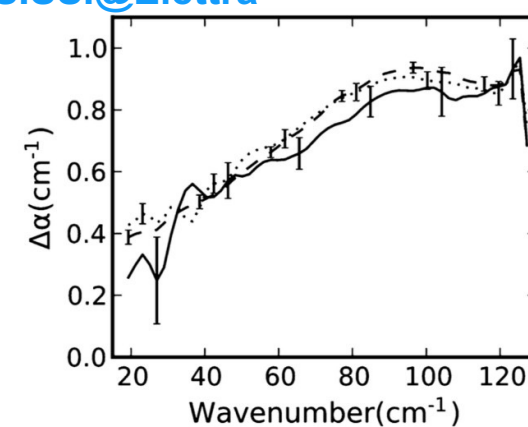
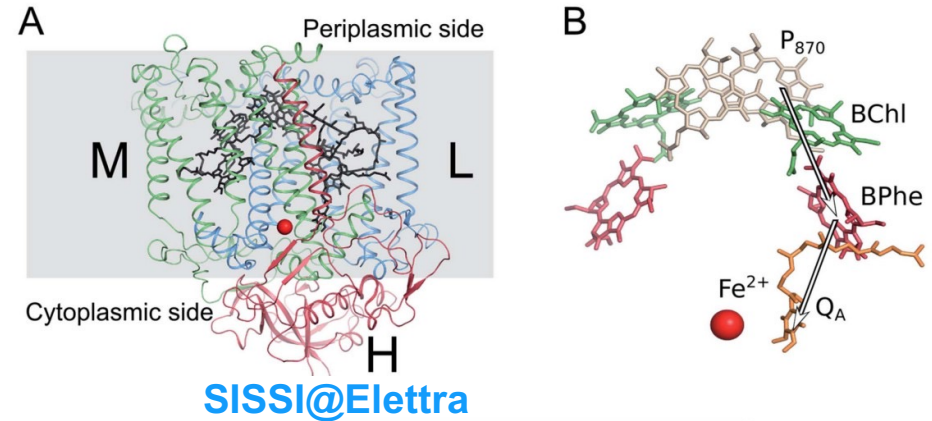
THz Spectroscopy of proteins



SISSI@Elettra



F. Piccirilli et al., Biophysical Chemistry 2015



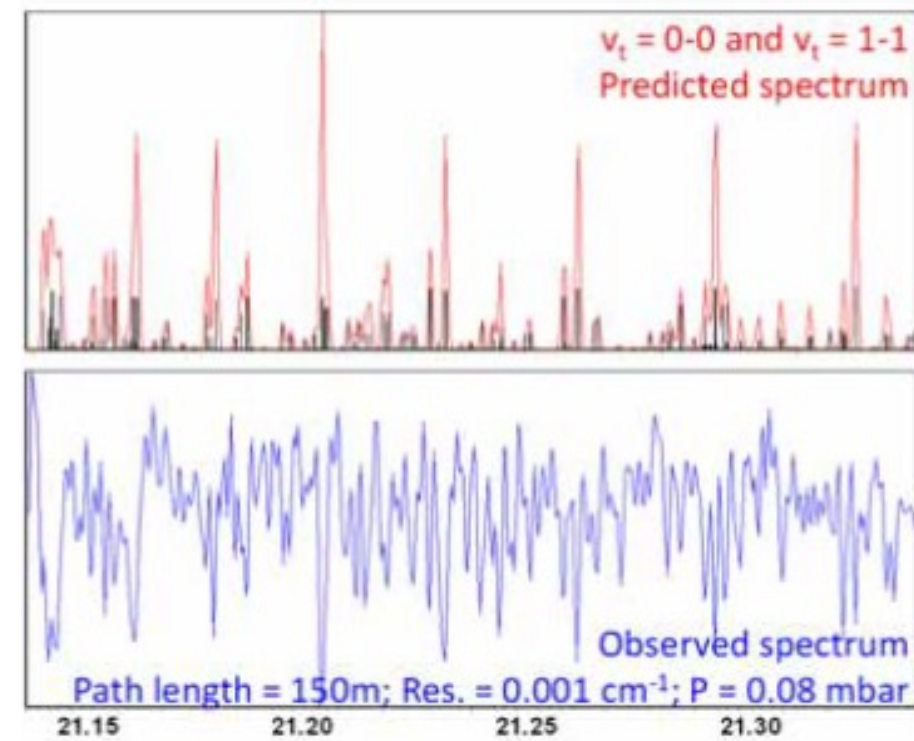
I. Lundholm et al., RSC Adv. 2014



High Resolution Spectroscopy

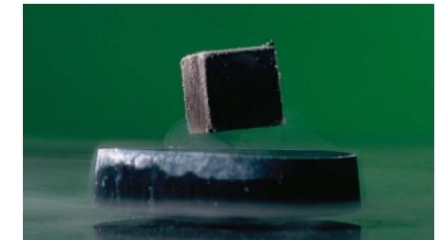


*Detecting molecular rotation and
rovibration transitions in gas*
SOLEIL

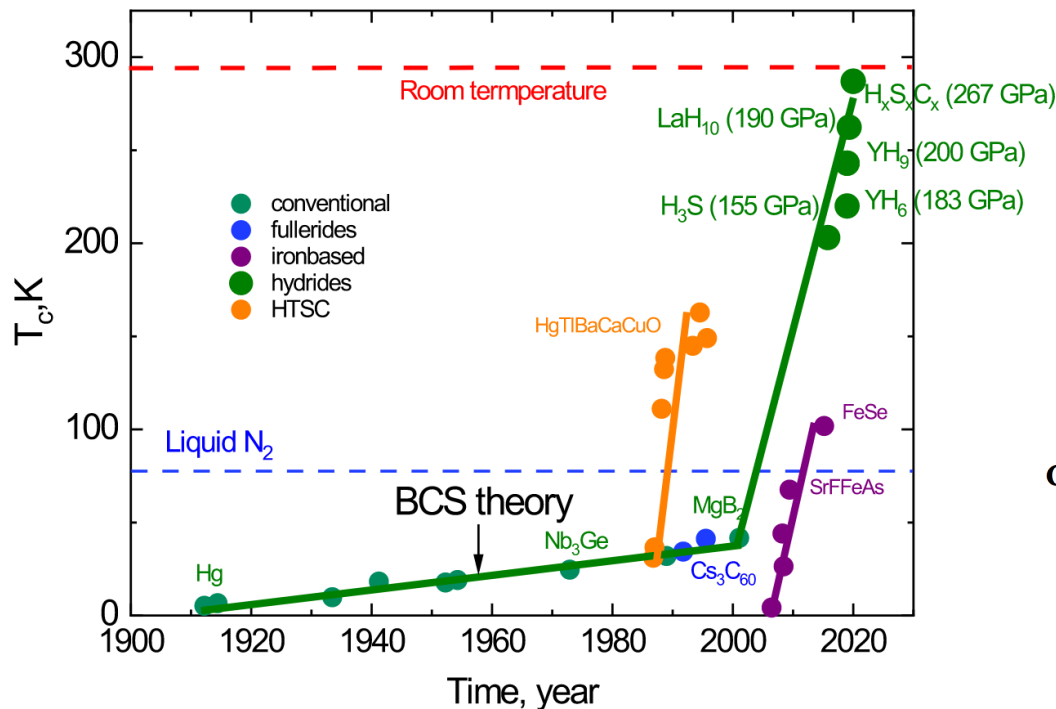


J.-B. Brubach et al., 2010

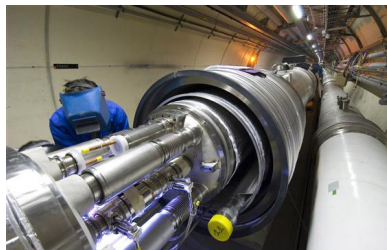
Superconductivity



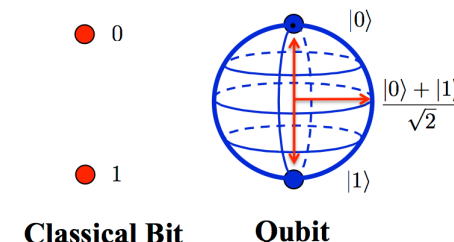
Boeri et al., 2022



Accelerators



Quantum computing



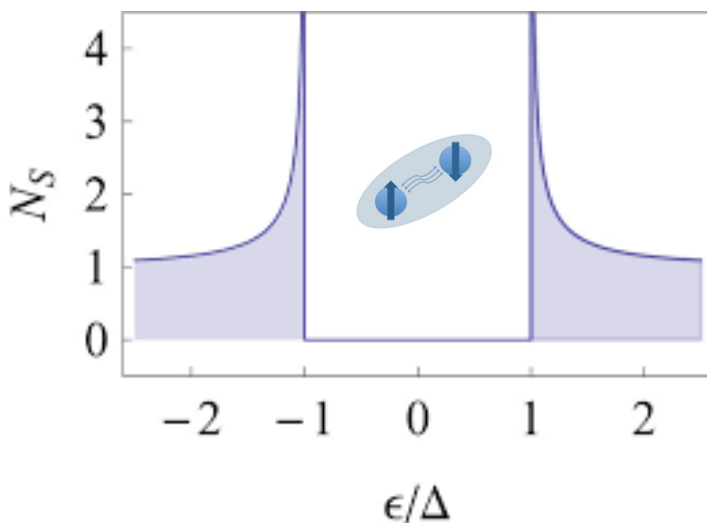
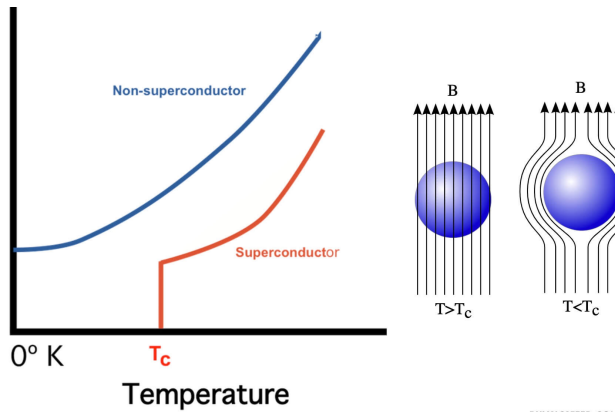
Magnetic levitation trains (Maglev)



NMR



BCS Superconductivity

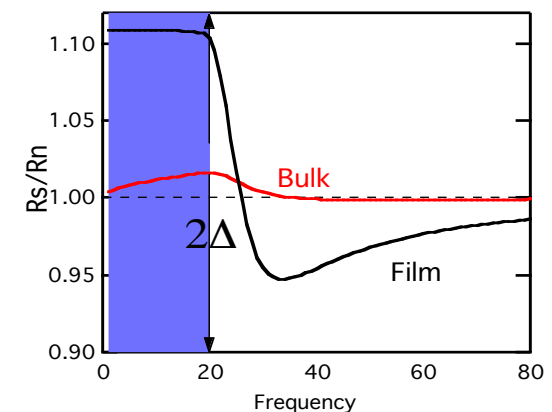
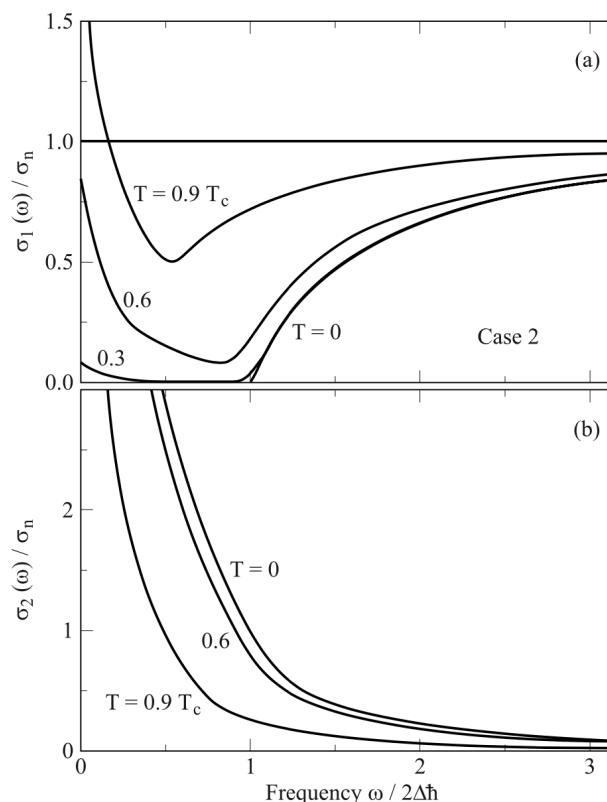


$$g(E) = \frac{(E^2 + \Delta^2 + \hbar\omega E)}{(E^2 - \Delta^2)^{1/2}((E + \hbar\omega)^2 - \Delta^2)^{1/2}}$$

$$\Delta \approx \hbar\omega_D e^{-2/N(0)V}$$

$$2\Delta/k_B T_C = 3.52 \quad \rightarrow \quad T_c \approx 10 \text{ K} \rightarrow 2\Delta \approx 1 \text{ THz}$$

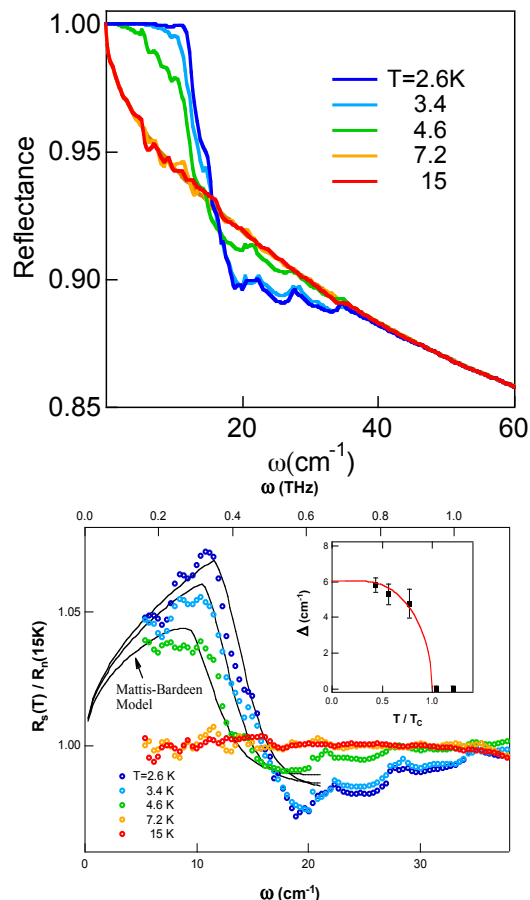
Mattis-Bardeen equations



BCS Superconductors

BESSY – low α

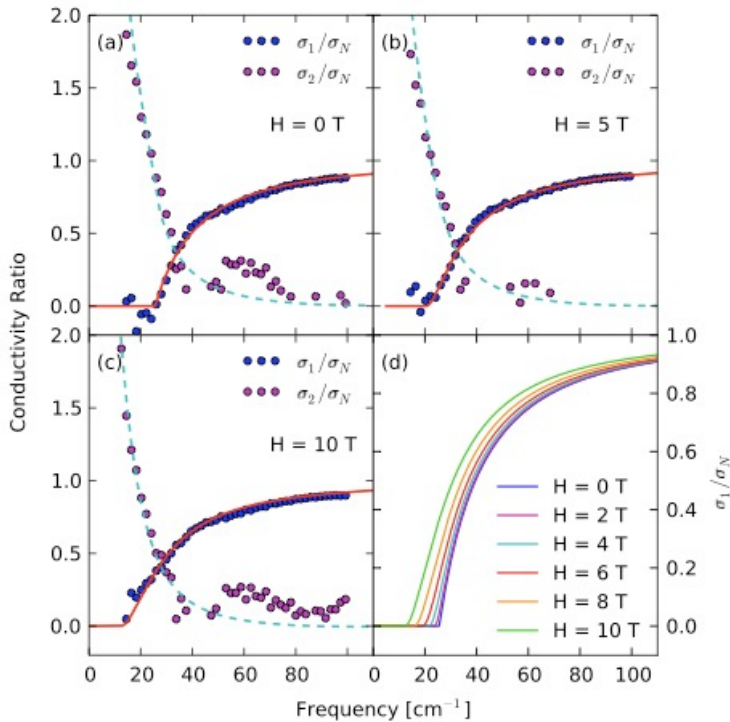
B-doped diamond



Ortolani et al., PRL (2006)

Brookhaven

Nb_{0.5}Ti_{0.5}N



Xi et al., PRL (2011)



Outline

The THz spectral range

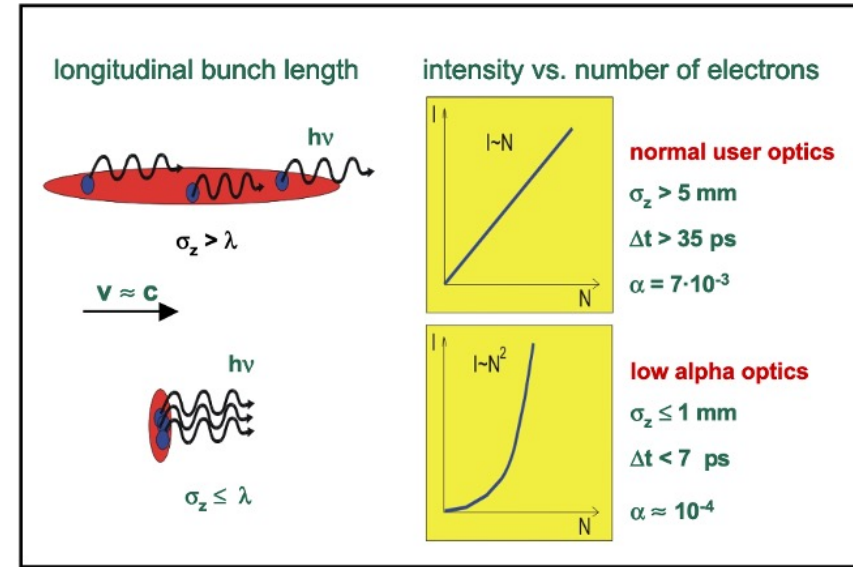
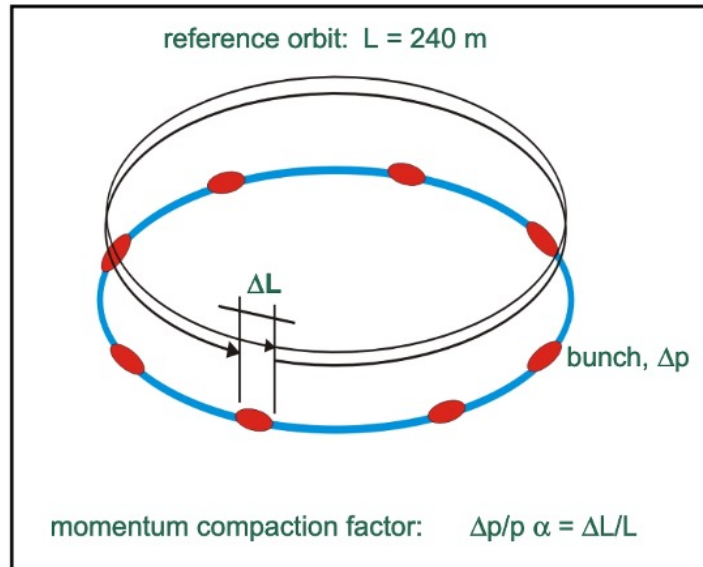
THz spectroscopy with Synchrotron Radiation

Accelerator-based Coherent sources of THz light

TeraFERMI – the THz beamline at FERMI

THz studies with FELs

Coherent Synchrotron Radiation

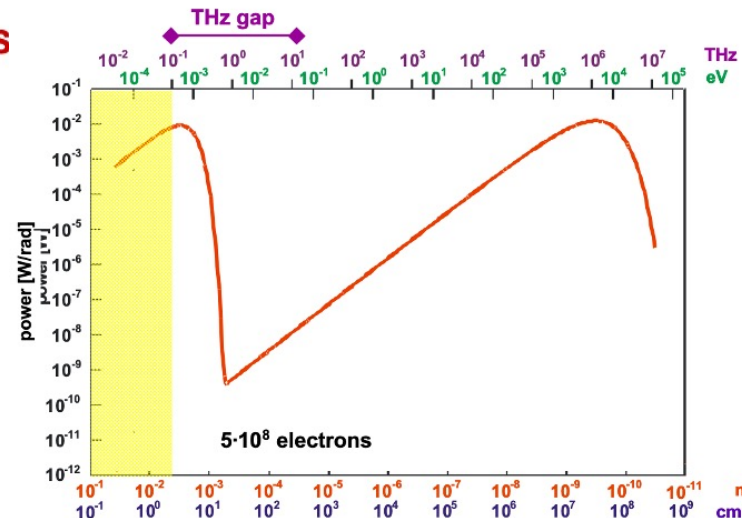


Dedicated Machine Mode: “Low α “ Optics at BESS

- Bunch shortening down to and below the mm-range
- Emission in the FIR range is drastically enhanced:

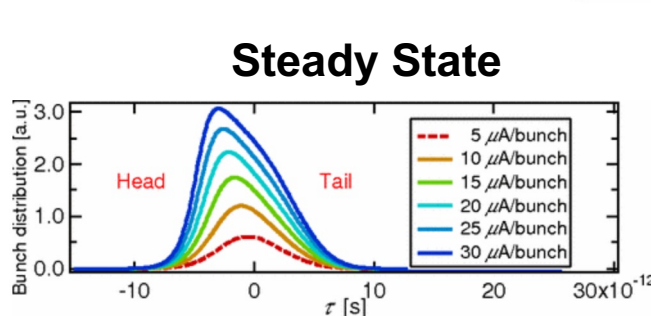
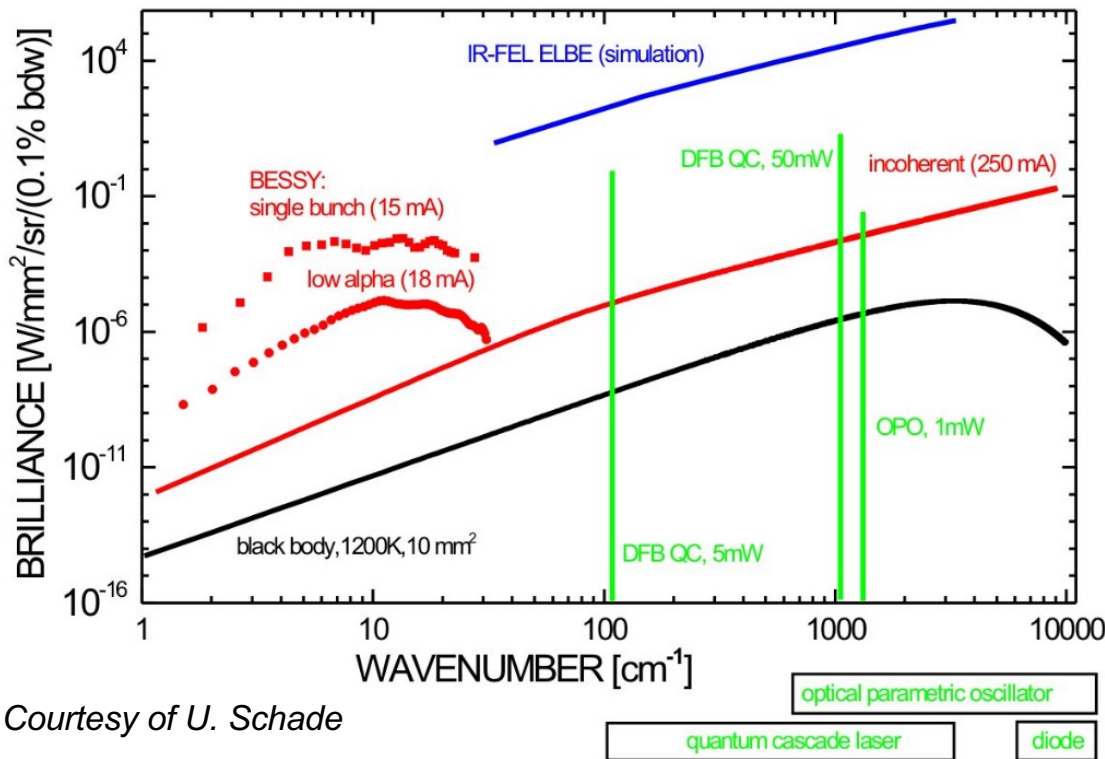
$$I = I_{incoh} + I_{coh} = Ni(1 + Nf_v)$$

$$f_v = \left| \int n(z) e^{i\pi \cos(\theta) z} dz \right|^2$$



Courtesy of U. Schade

Coherent Synchrotron Radiation



Sannibale et al., PRL 2004

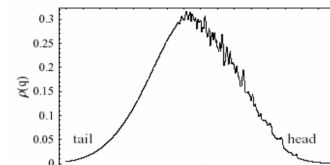
“bursting” mode

- high power CSR
- very noisy
- energy range: 2 - 50 cm^{-1}
- gain of $\sim 10^8$

“steady state” mode

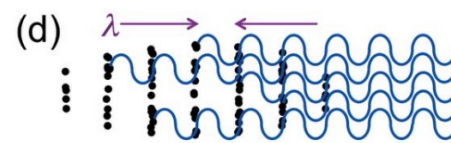
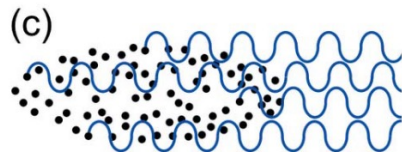
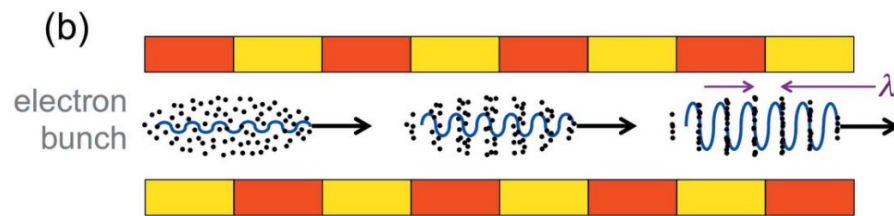
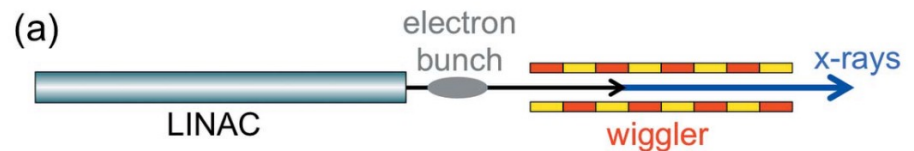
- low noise CSR
- energy range: 2 - 30 cm^{-1}
- gain of $\sim 10^4$

Bursting



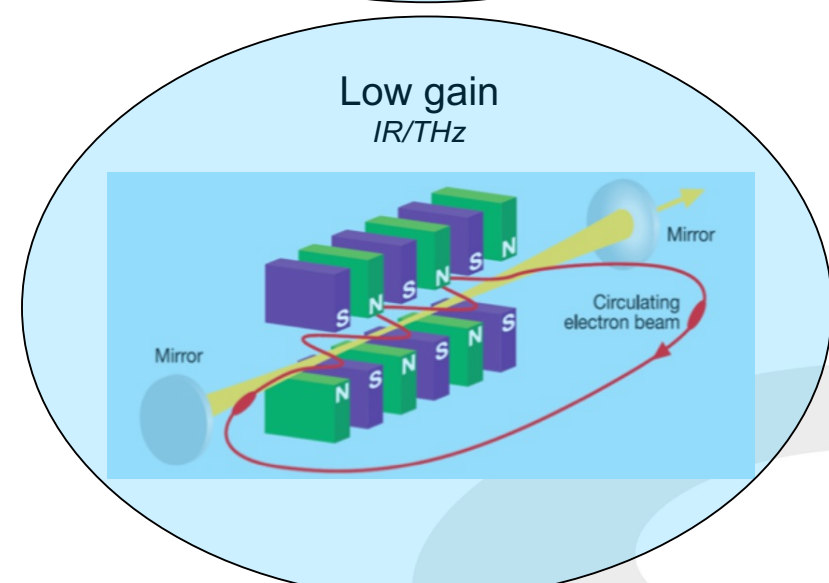
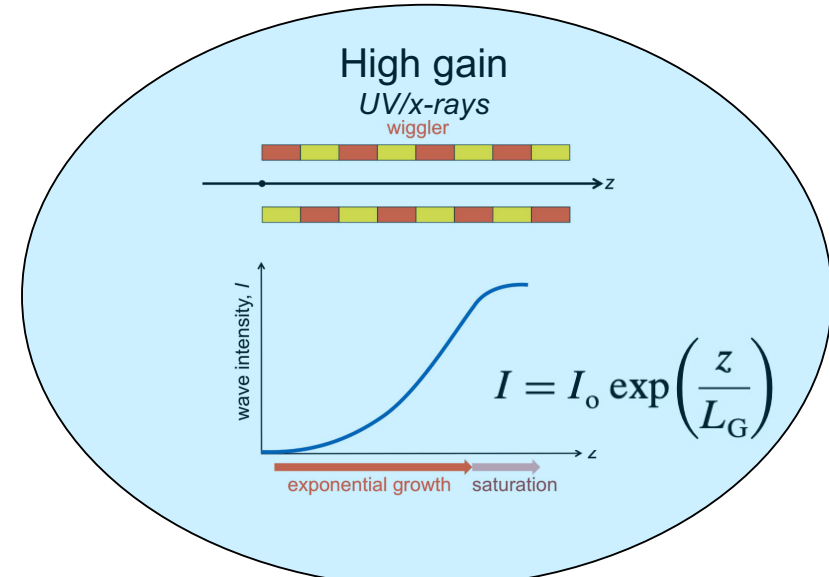
Simulated instability showing the microbunching.
Venturini, Warnock SLAC

Microbunching and free-electron-lasers



Ponderomotive force

$$f_p = eB_w v_T$$



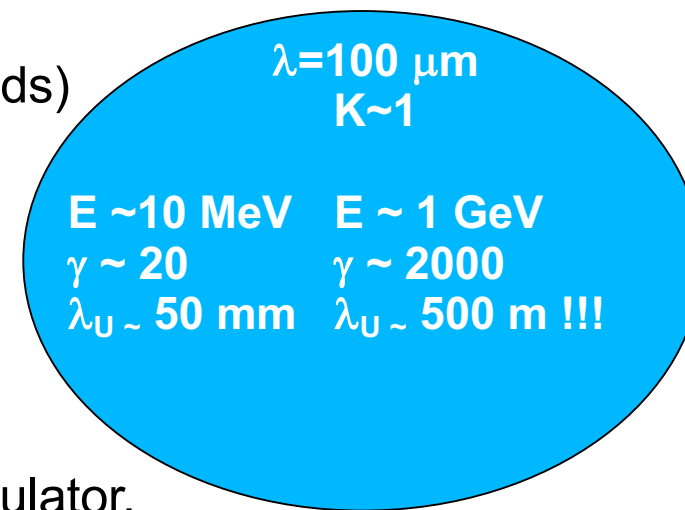
Hwu and Margaritondo, JSR 2021

IR/THz low gain free-electron-lasers

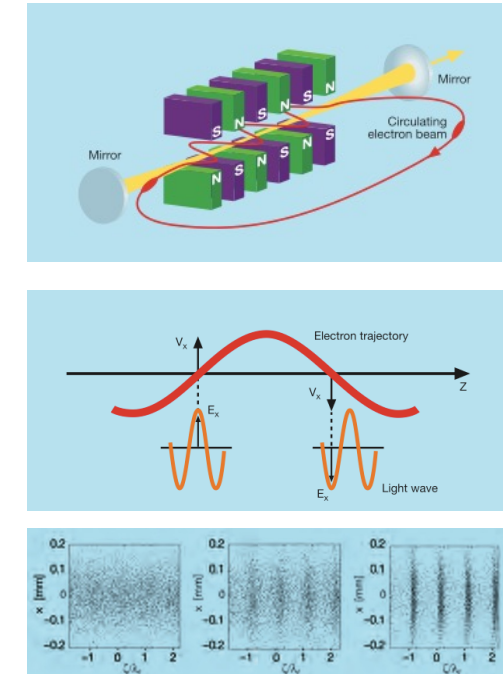
Low-gain FELs with optical cavity

- UCSB (USA)
- Budker Institute (Russia)
- CLIO (France)
- FELIX / FLARE (Netherlands)
- FELBE (Germany)
- ...

$$\lambda = \frac{\lambda_u}{2\gamma^2} \left(1 + \frac{K^2}{2} \right)$$

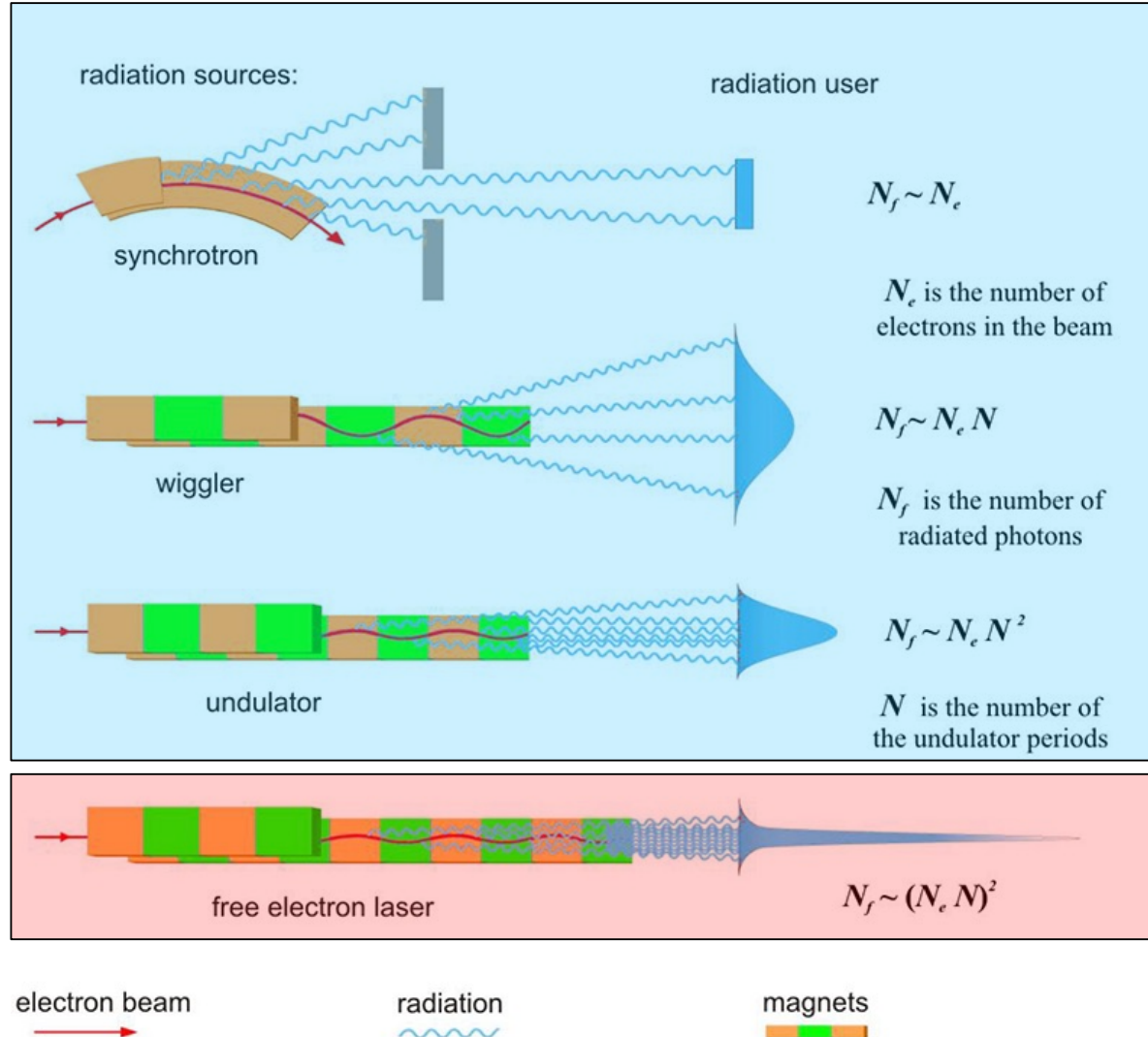


Upon one passage in the undulator,
radiation grows by a few percent
→ Several passages are needed
before reaching saturation



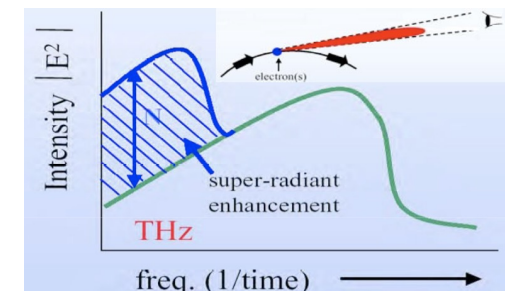
From DESY-FLASH brochure

... a recap



Incoherent

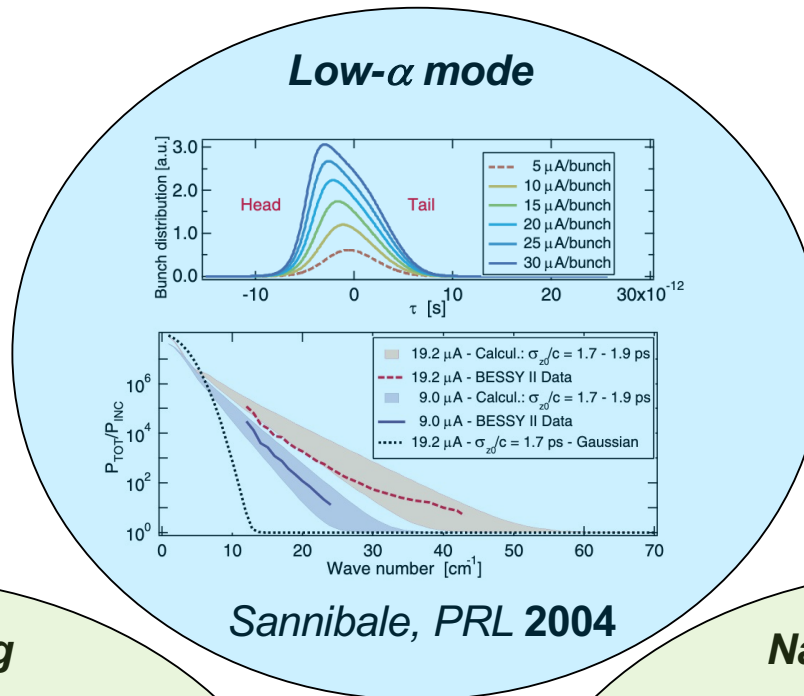
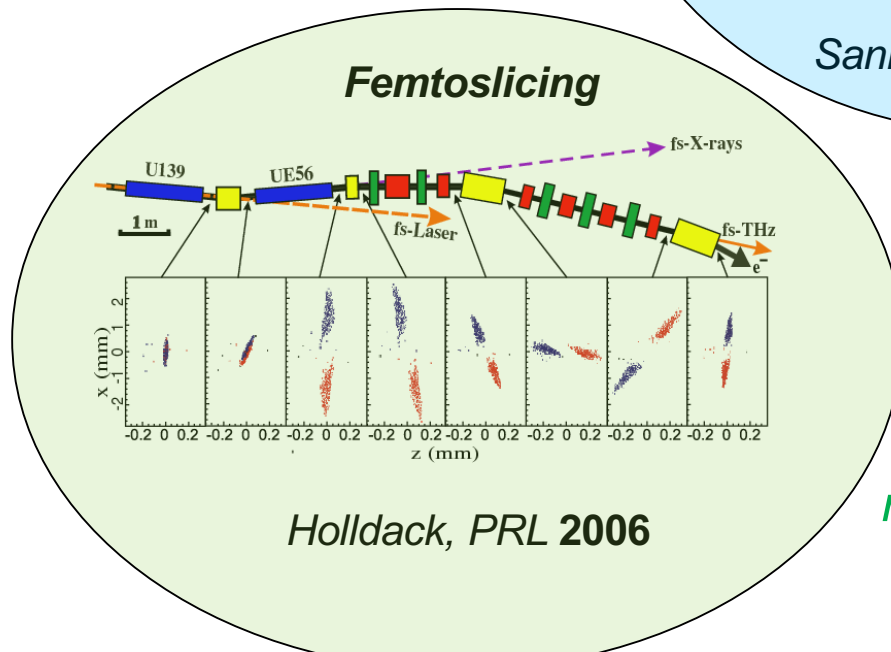
Can be made coherent through **superradiance**



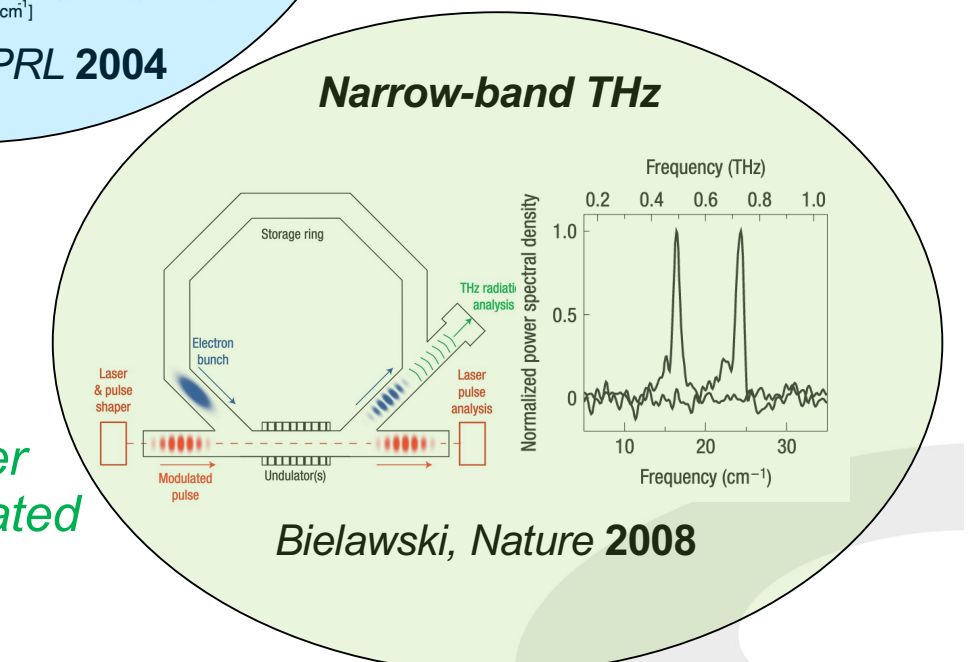
$$f_v = \left| \int n(z) e^{i\pi \cos(\theta) z} dz \right|^2$$

Coherent

THz superradiant sources in SRs



Beam shaping through Magnetic lattice
...but CSR wakefields play a role!



Laser modulated

THz superradiant sources in LINACs

$$I = I_{incoh} + I_{coh} = Ni(1 + Nf_v)$$

$$f_v = \left| \int n(z) e^{i\pi \cos(\theta)z} dz \right|^2$$

$$A_f = \frac{I_{coh}}{I_{incoh}} = Nf_v$$

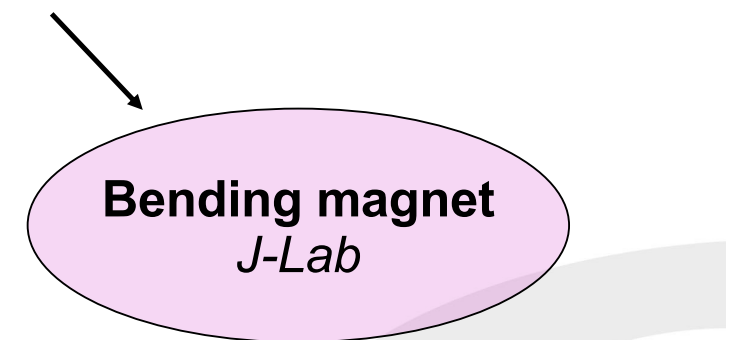
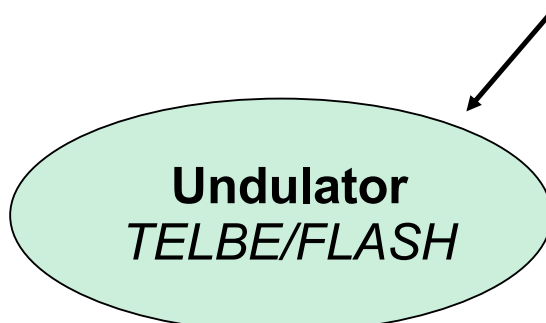
$$1 \text{ C} = 6,241 \cdot 10^{18} \text{ e}$$

For Storage Rings:

$\sim 1 \text{ pC/bunch} \rightarrow N \sim 6 \cdot 10^6 \rightarrow E \sim 10^{-10} \text{ J/pulse}$

For linear accelerators:

$\sim 1 \text{ nC/bunch} \rightarrow N \sim 6 \cdot 10^9 \rightarrow E \sim 10^{-4} \text{ J/pulse}$





Outline

The THz spectral range

THz spectroscopy with Synchrotron Radiation

Accelerator-based Coherent sources of THz light

TeraFERMI – the THz beamline at FERMI

THz studies with FELs

The FERMI seeded FEL

nature
photronics

PUBLISHED ONLINE: 23 SEPTEMBER 2012 | DOI: 10.1038/NPHOTON.2012.233

ARTICLES

Highly coherent and stable pulses from the
FERMI seeded free-electron laser in the
extreme ultraviolet → 100-20 nm

First user exp. Dec 2012

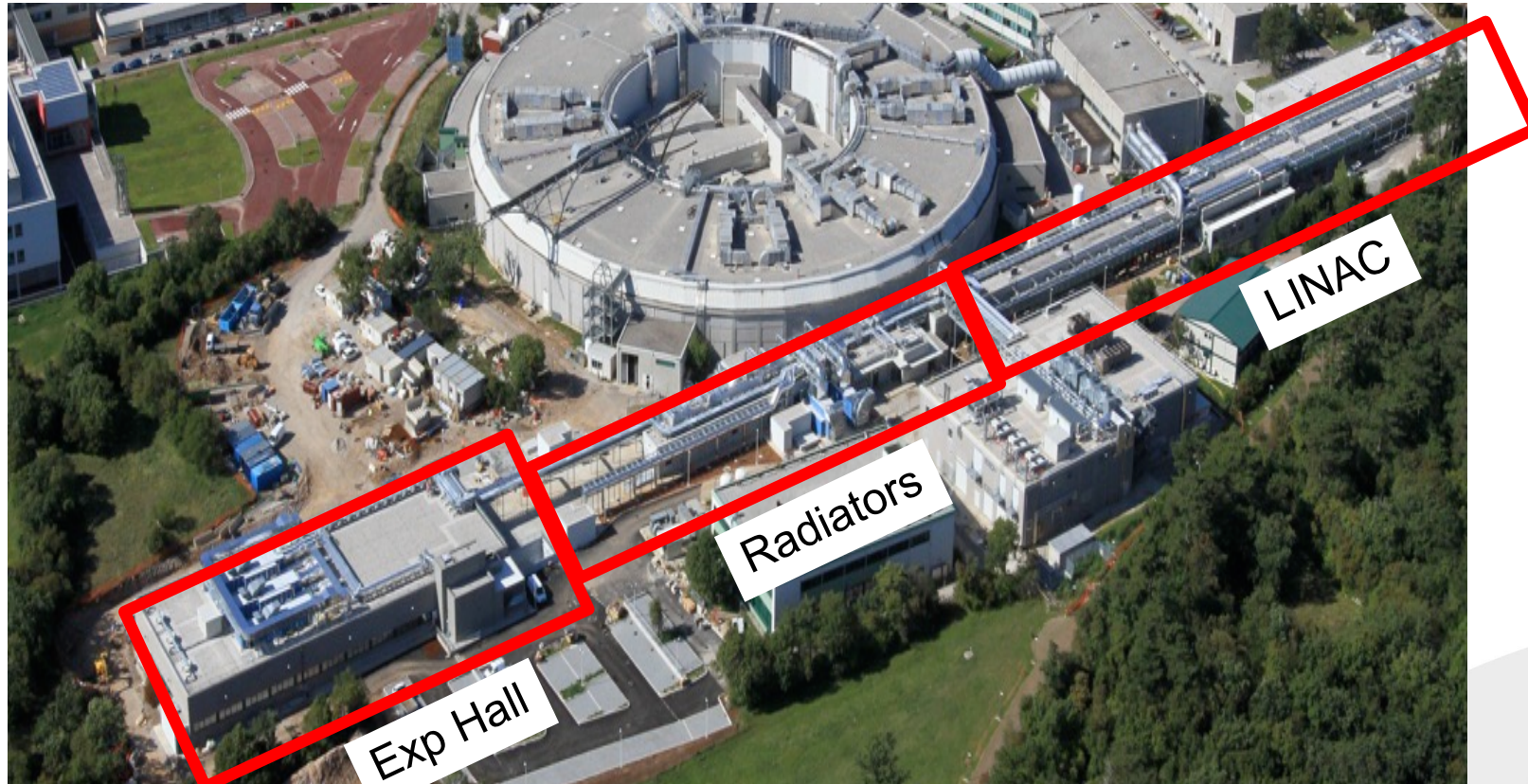
nature
photronics

PUBLISHED ONLINE: 20 OCTOBER 2013 | DOI: 10.1038/NPHOTON.2013.277

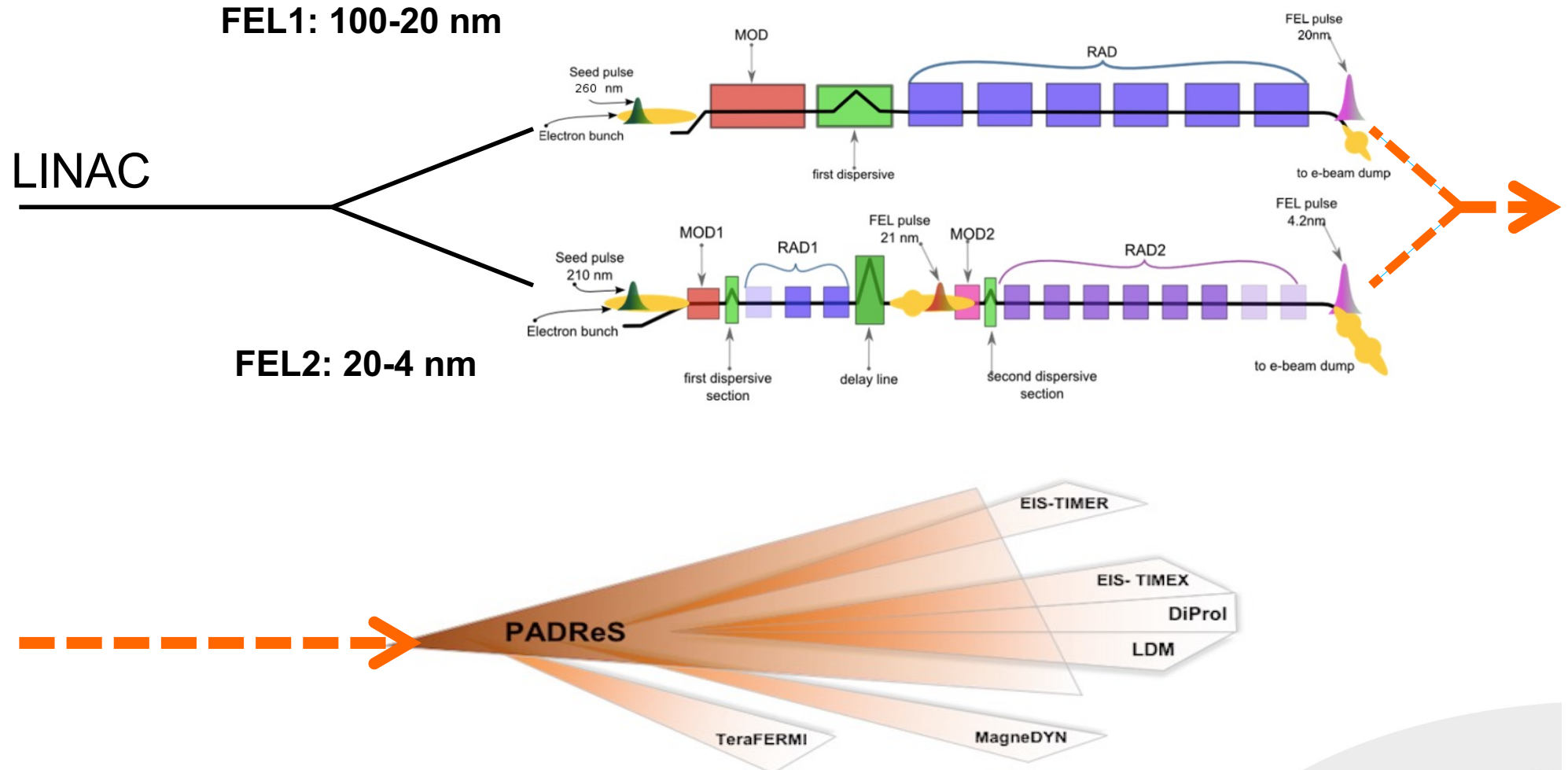
ARTICLES

Two-stage seeded soft-X-ray free-electron laser → 20-4 nm

First user exp. July 2016

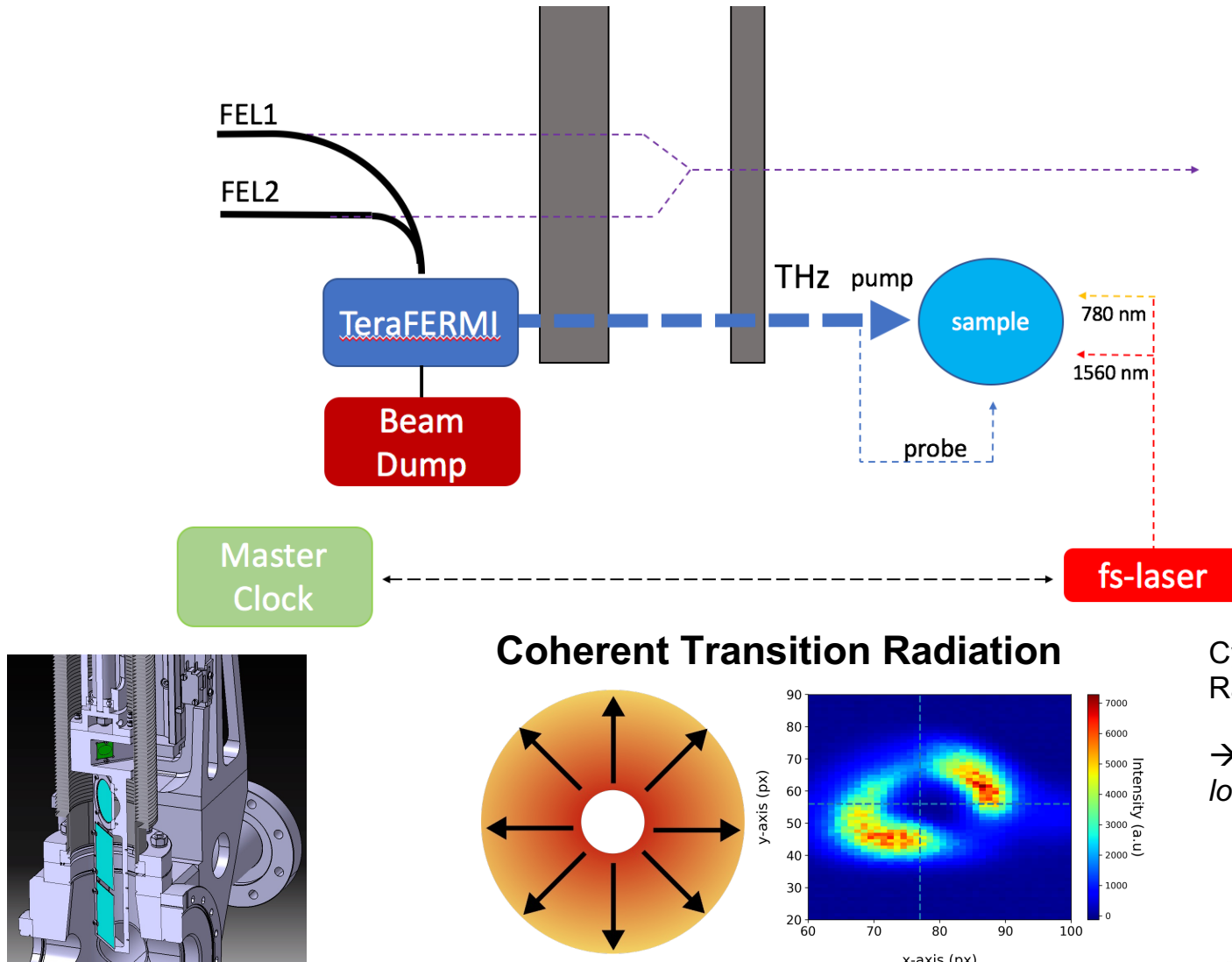


The FERMI seeded FEL

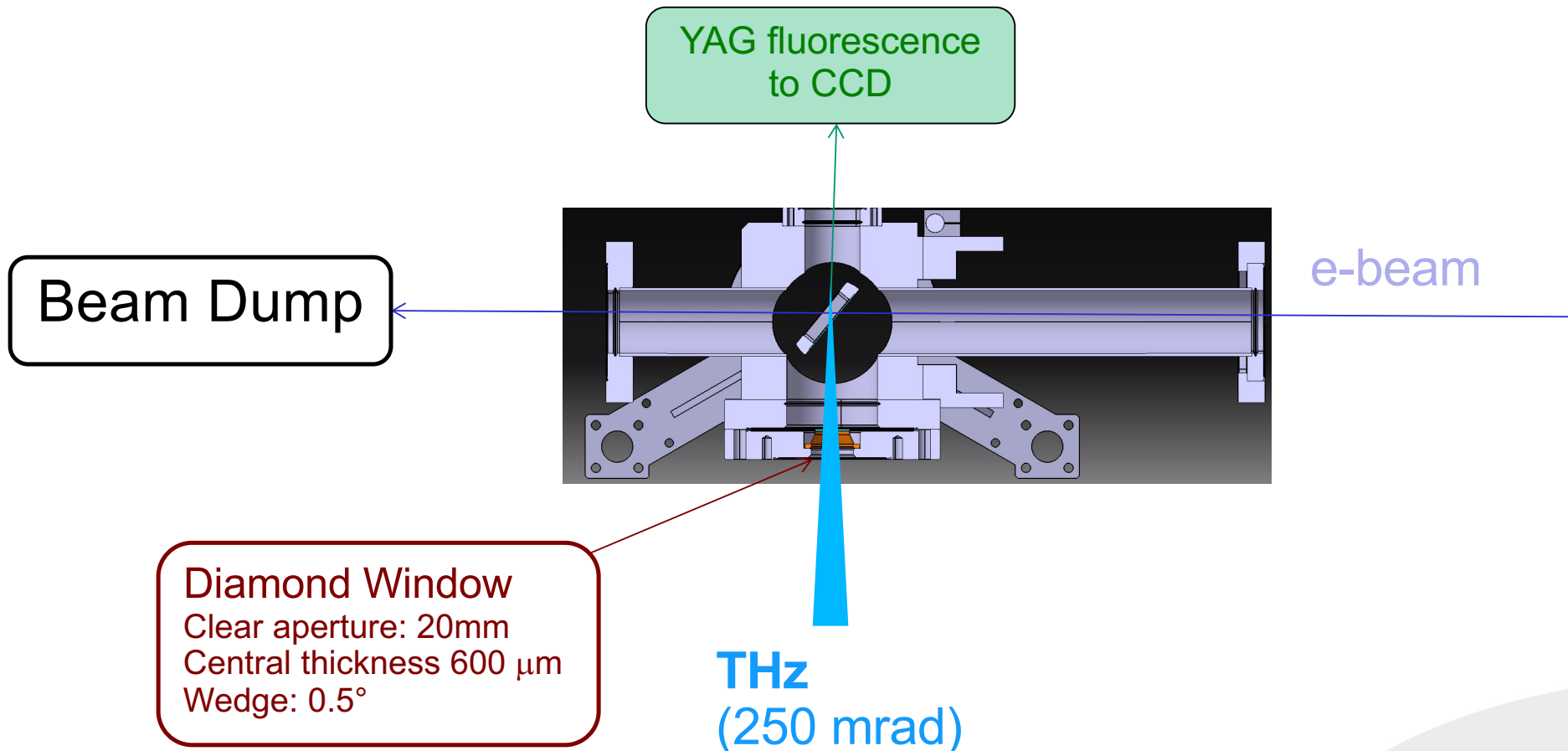




The TeraFERMI beamline



TeraFERMI Source

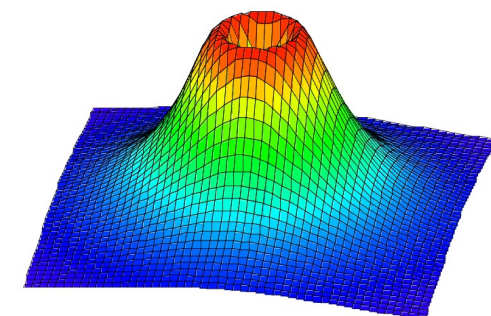
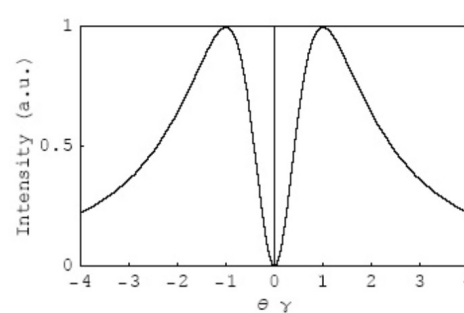


Transition Radiation

Transition Radiation occurs when relativistic electrons cross the boundary between two media of different dielectric constant

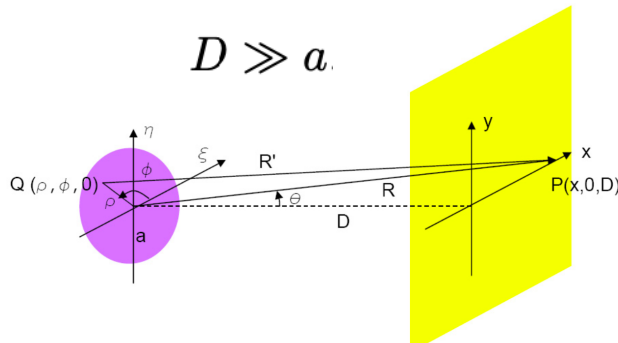
The Ginzburg-Frank equation:

$$\frac{d^2U}{d\omega d\Omega} = \frac{e^2}{4\pi^3 \epsilon_0 c} \frac{\beta^2 \sin^2 \theta}{(1 - \beta^2 \cos^2 \theta)^2}$$



$$\theta_{max} = \arcsin\left(\frac{\sqrt{1-\beta^2}}{\beta}\right) = \arcsin\left(\frac{1}{\beta\gamma}\right) \simeq \frac{1}{\gamma} \quad \text{for } \gamma \gg 1$$

**Generalized Ginzburg-Frank equation
(TR from finite screen, far-field)**



Casalbuoni, TESLA Report 2005-15

$$\frac{d^2U}{d\omega d\Omega} = \frac{e^2}{4\pi^3 \epsilon_0 c} \cdot \frac{\beta^2 \sin^2 \theta}{(1 - \beta^2 \cos^2 \theta)^2} [1 - T(\theta, \omega)]^2$$

with

$$T(\theta, \omega) = \frac{\omega a}{c\beta\gamma} J_0\left(\frac{\omega a \sin \theta}{c}\right) K_1\left(\frac{\omega a}{c\beta\gamma}\right) + \frac{\omega a}{c\beta^2\gamma^2 \sin \theta} J_1\left(\frac{\omega a \sin \theta}{c}\right) K_0\left(\frac{\omega a}{c\beta\gamma}\right)$$



Outline

The THz spectral range

THz spectroscopy with Synchrotron Radiation

Accelerator-based Coherent sources of THz light

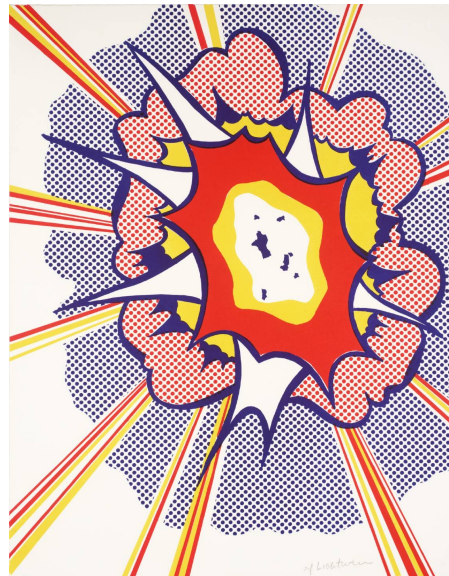
TeraFERMI – the THz beamline at FERMI

THz studies with FELs

THz pumping

THz radiation is non-ionizing, highly penetrating, and provides high chemical specificity

THz light couples to electronic, vibrational and magnetic excitations



Optical pump



THz pump

THz control of matter

Nucleae/lattice

Nonlinear phonics
Macromolecules
Molecular alignment
Reaction pathways

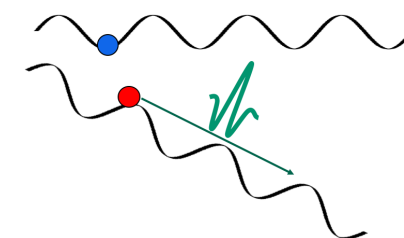
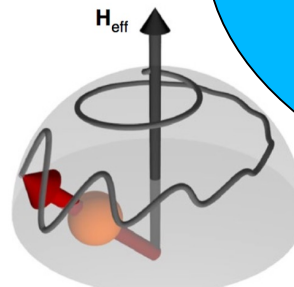
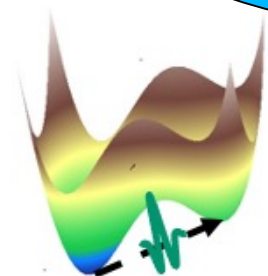
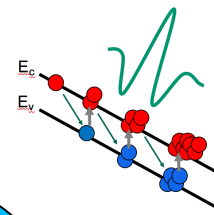
Electrons

Impact ionization
Intervalley scattering
Zener tunneling
Franz-Keldysh

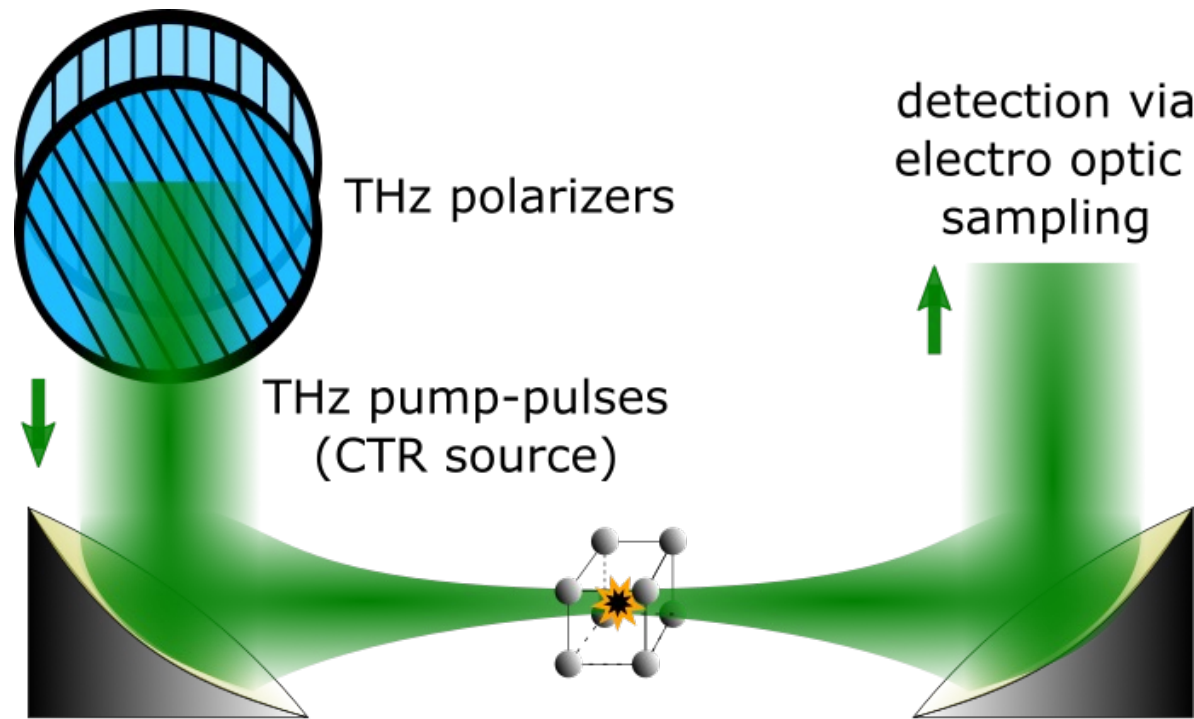
Spins

Ultrafast magnetic switching
Precession

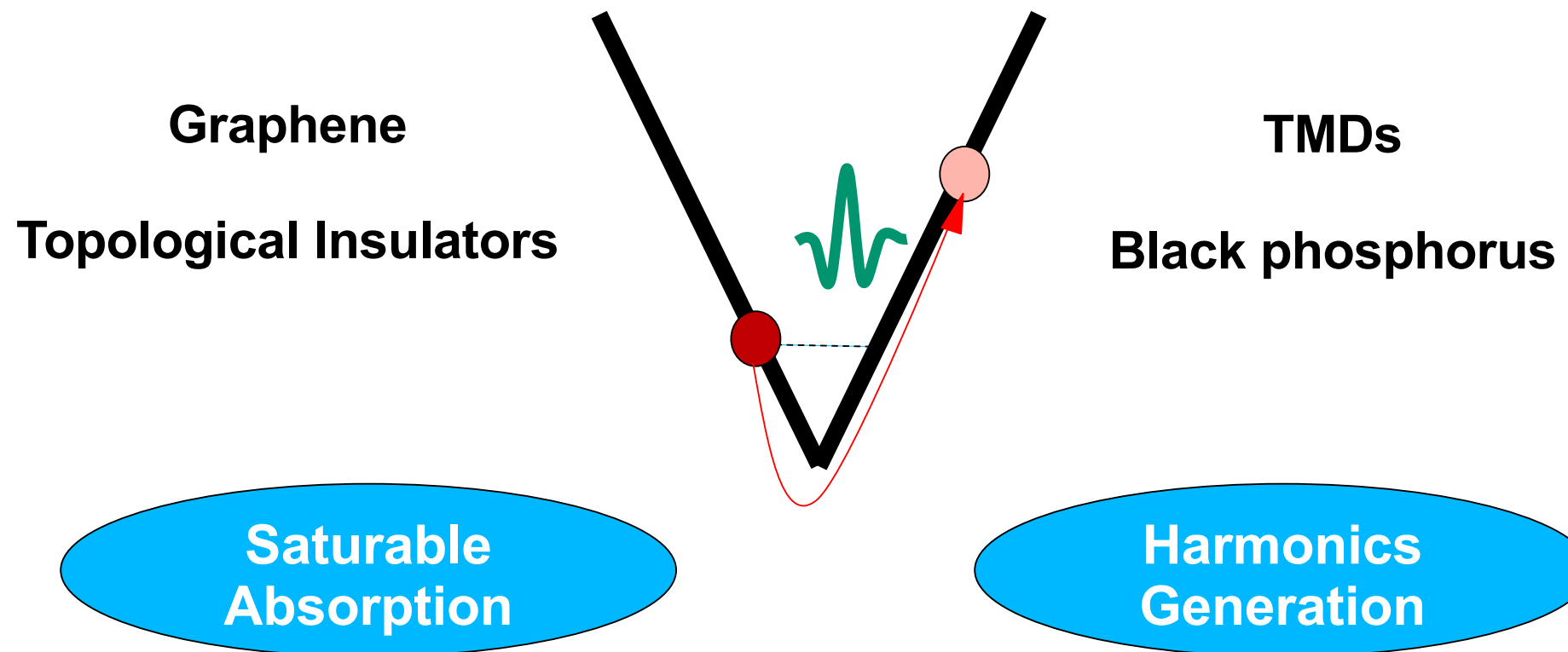
1 MV/cm \sim 0.3 Tesla



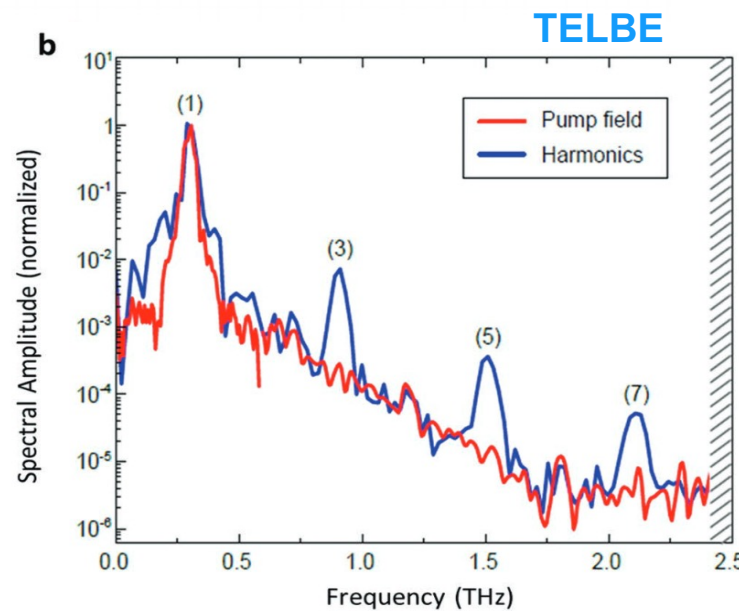
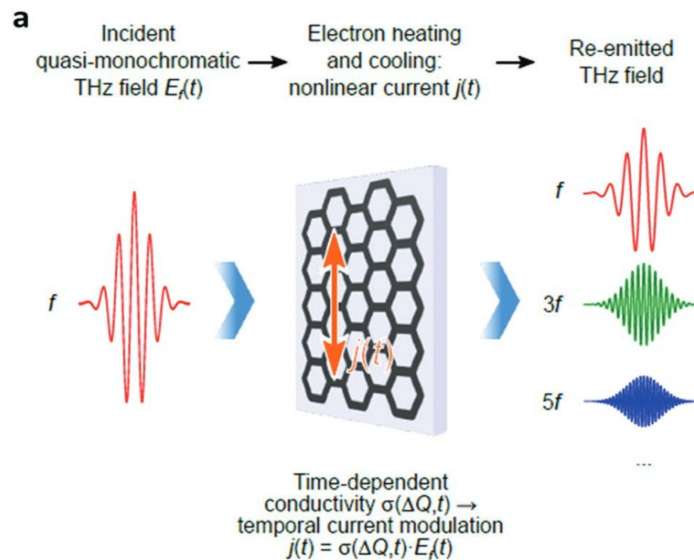
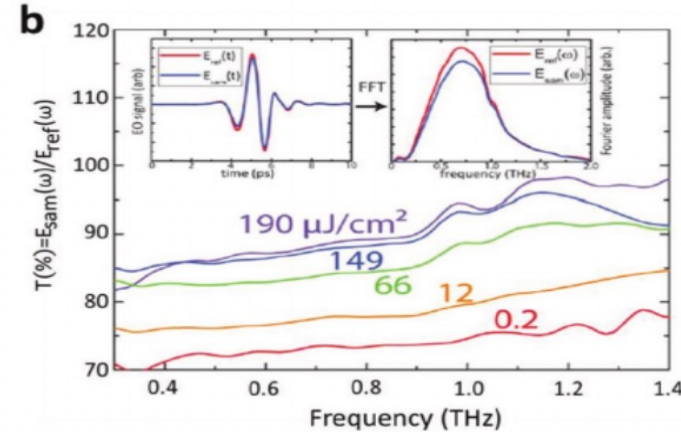
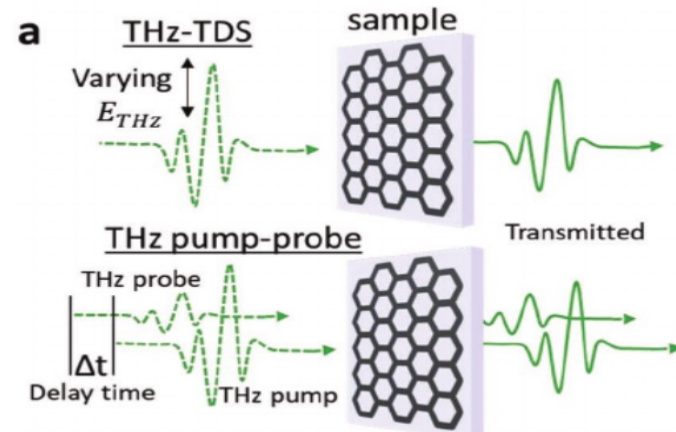
Fluence-dependent spectroscopy



Dirac materials

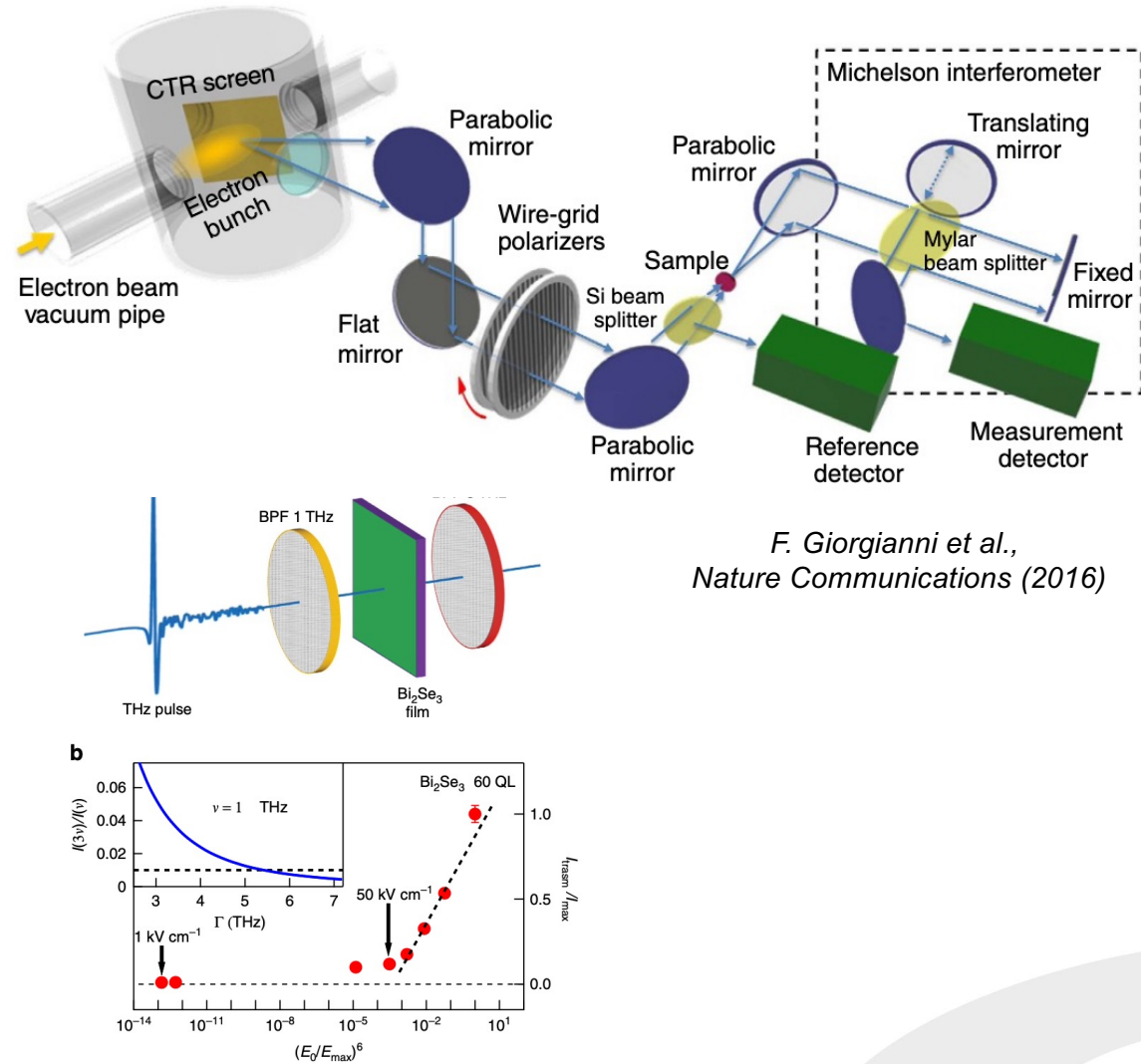
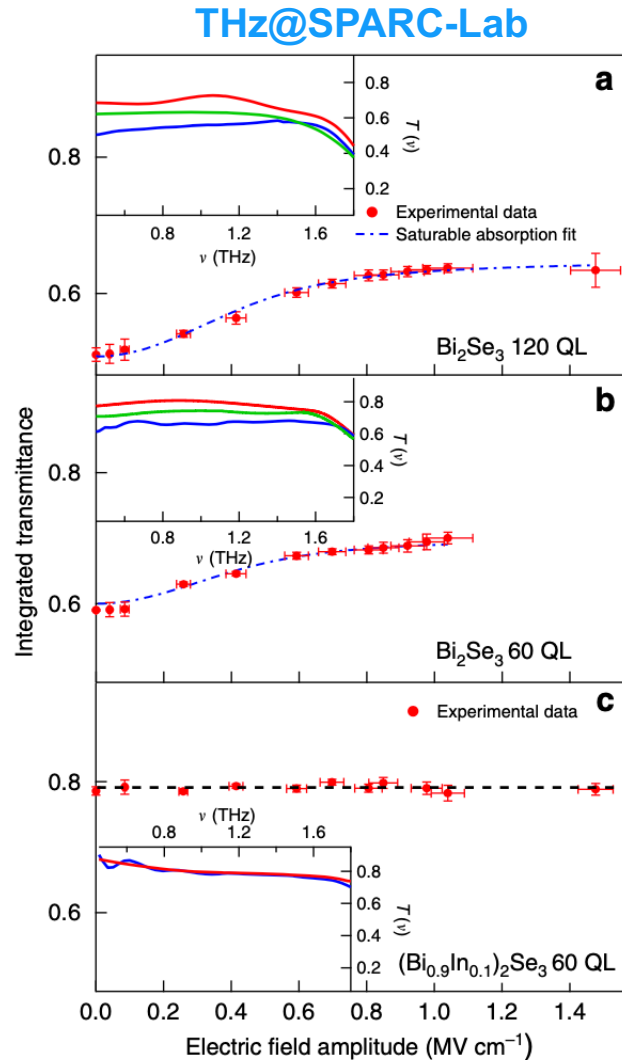


THz nonlinearities in graphene



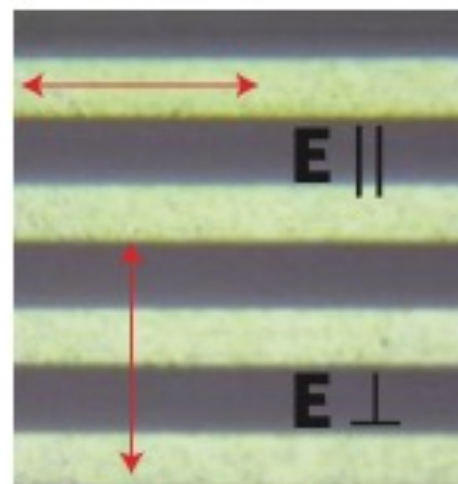
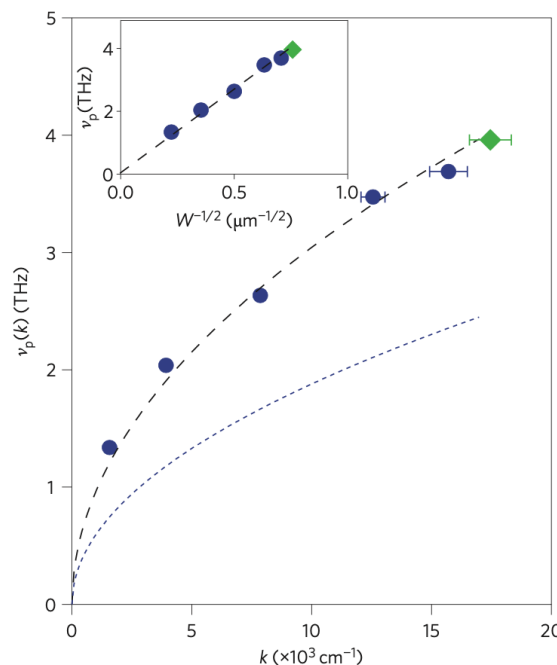
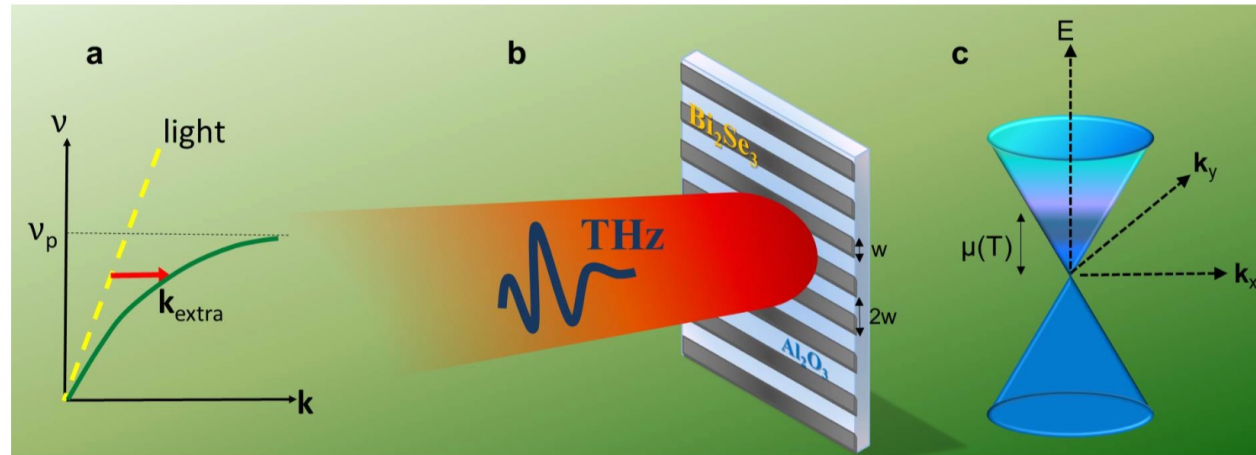
A. Hafez et al., Advanced Optical Materials (2022)

THz nonlinear properties of Bi_2Se_3

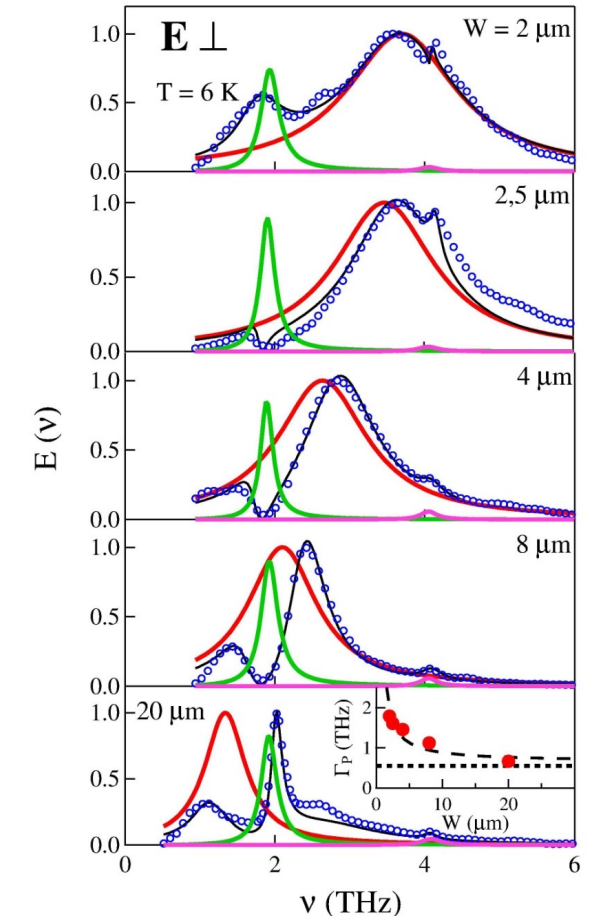


F. Giorgianni et al.,
Nature Communications (2016)

THz Plasmonics on Bi_2Se_3

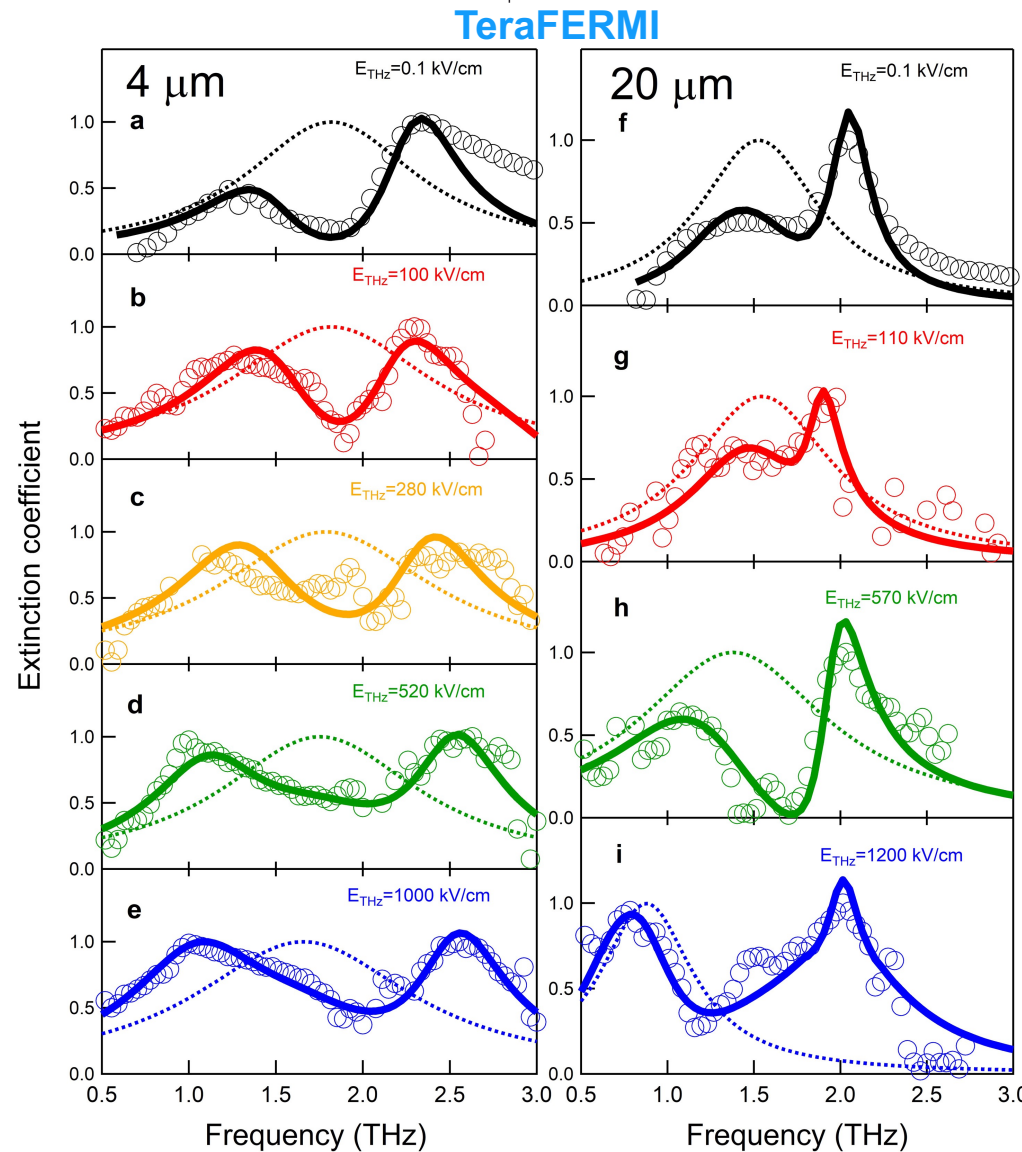


P. Di Pietro et al., Nature Nano. 2013

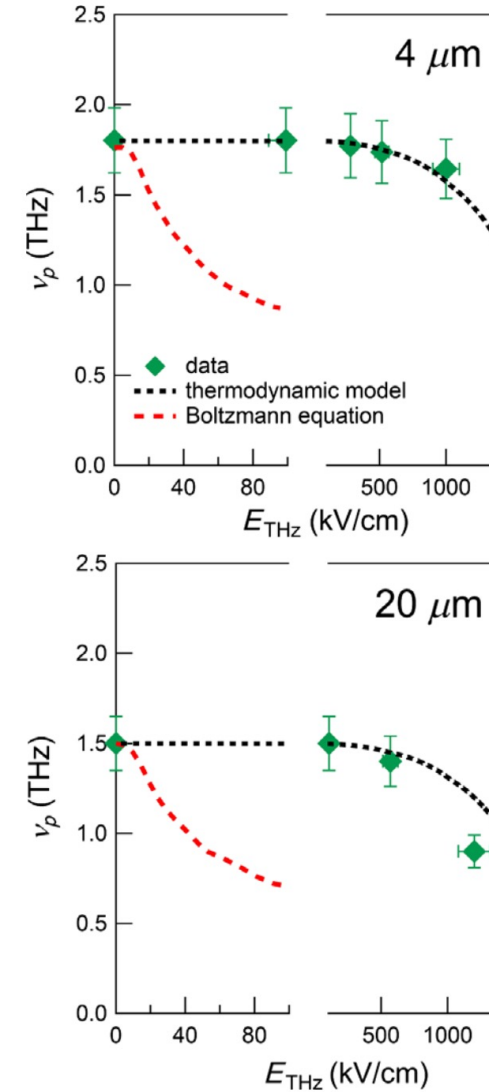


Fano fitting

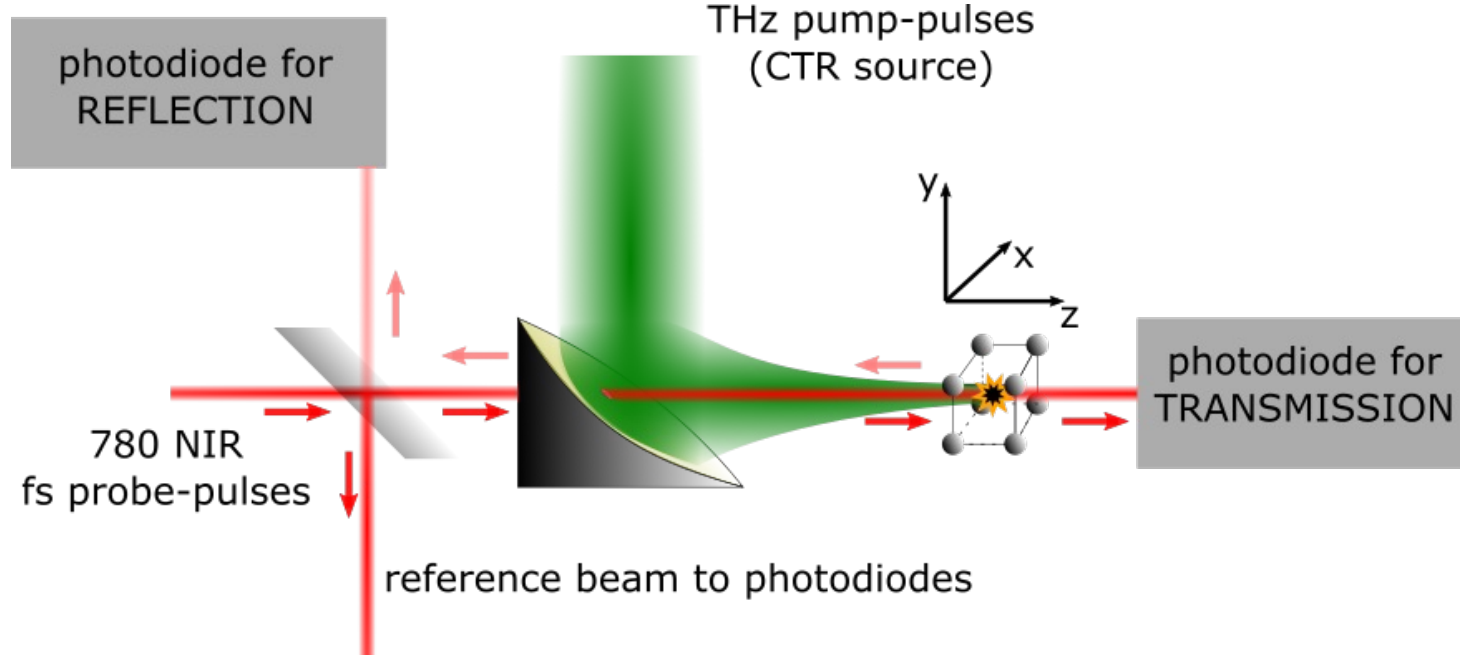
Fluence-dependent THz properties



P. Di Pietro et al., PRL 2020

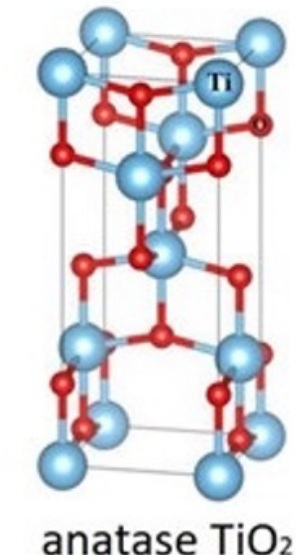
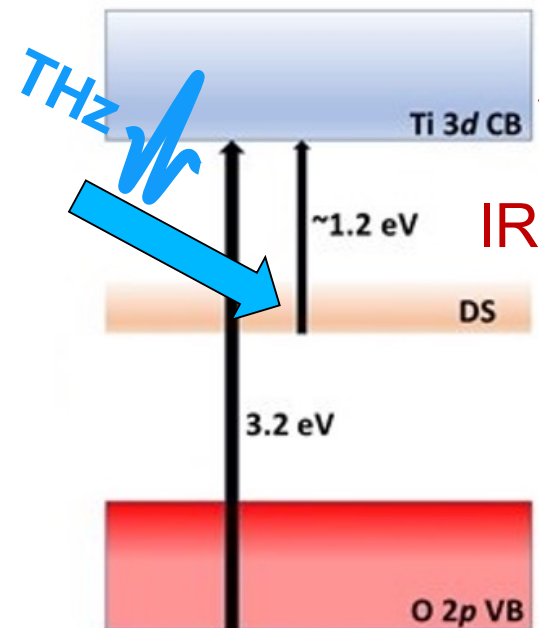


THz-pump/IR-probe



- Normal incidence geometry
- Simultaneous measurement of reflectance and transmittance
- Terahertz Kerr configuration also available

THz control of the O₂ defect state in TiO₂

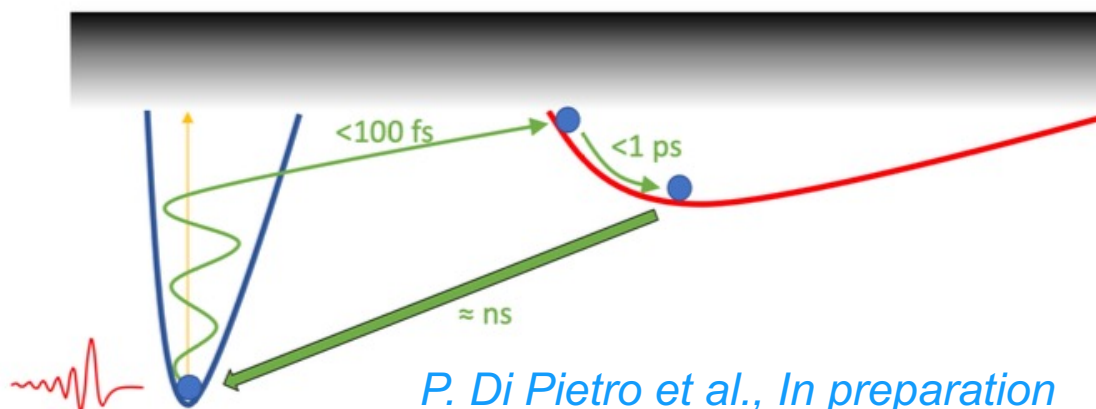
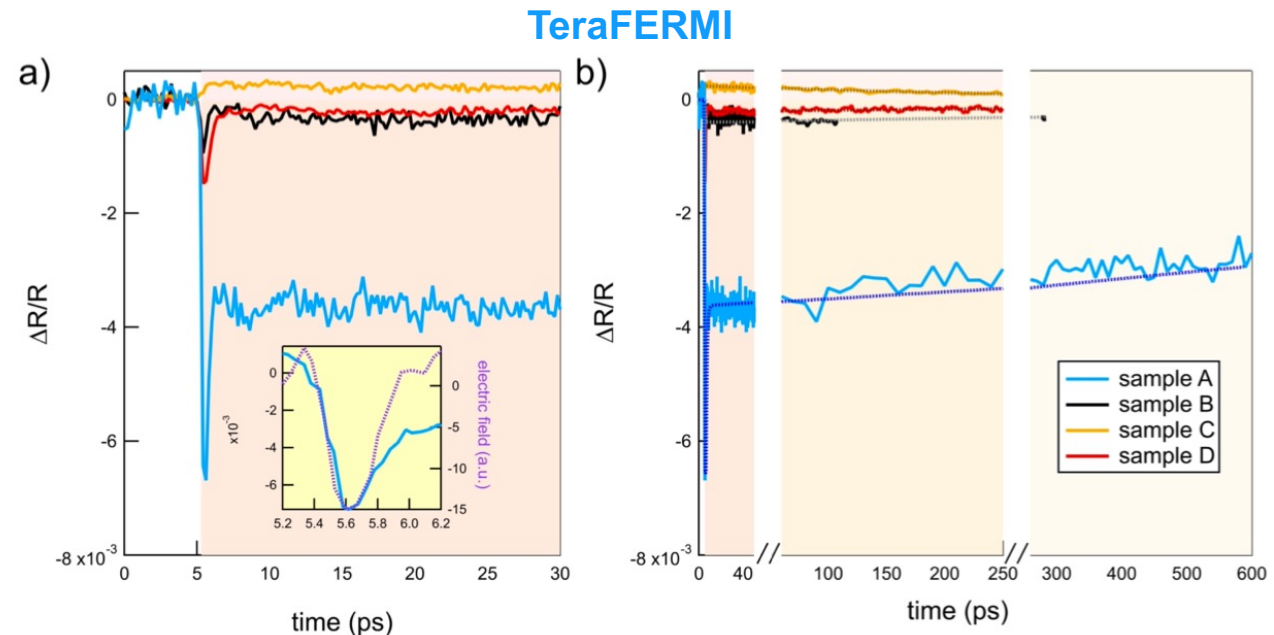
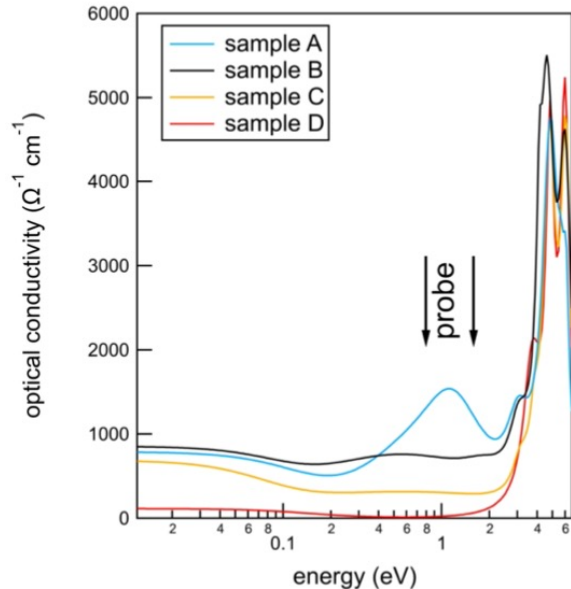


Chemical doping arising from oxygen vacancies induces the creation of in-gap defect states (DS)

ARPES measurements confirm the existence of both localized (IG) and delocalized (2DEG) electronic states with Ti³⁺ and Ti⁴⁺ character, respectively.

Using THz to control and modulate on ultrafast timescales the photoexcitation of the Defect State

THz control of the O₂ defect state in TiO₂

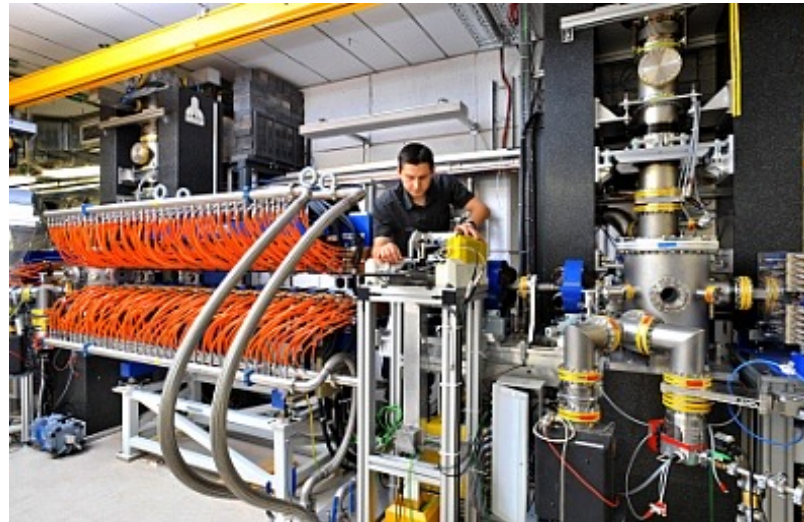




Elettra
Sincrotrone
Trieste

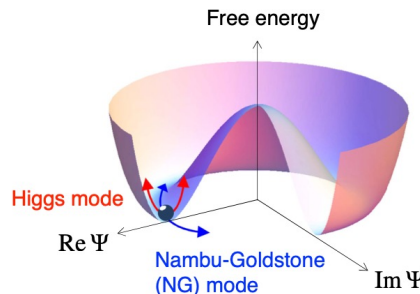
Narrowband THz

Superradiant undulator *TELBE*

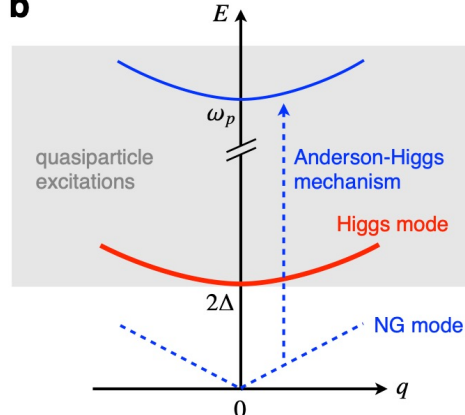


THz Higgs modes in superconductors

a



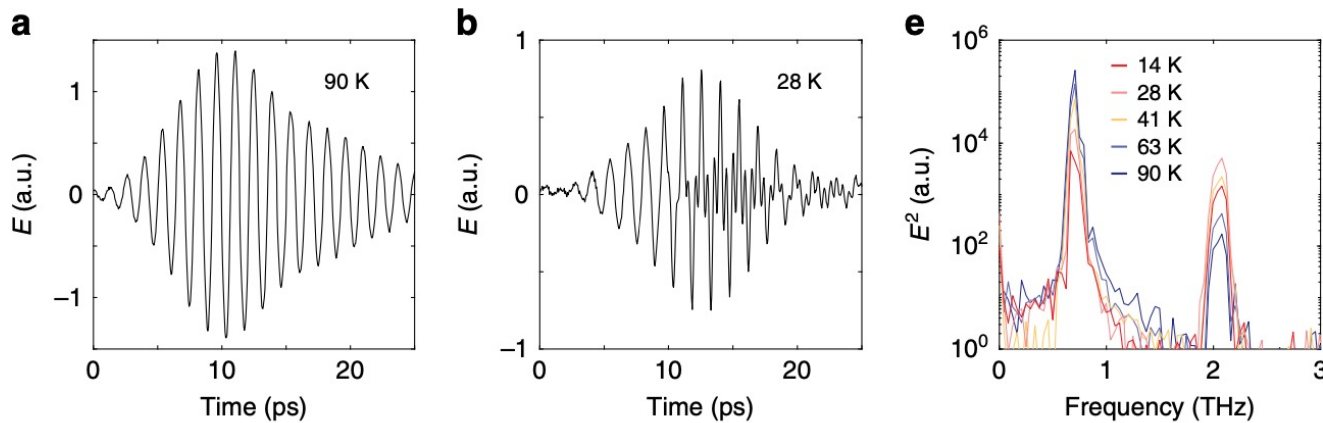
b



*The Higgs mode does not have any electric charge, electric dipole, magnetic moment, and other quantum numbers. Therefore it **does not couple** to external probes such as electromagnetic fields in the **linear-response regime**"*

R. Shimano & N. Tsuji, Ann. Rev. Cond. Mat. Phys. 2020

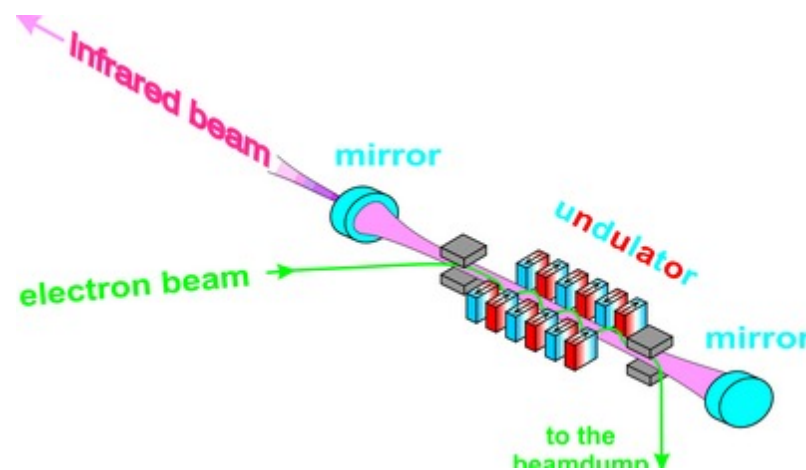
TELBE



H. Chu et al., Nat. Comm 2020

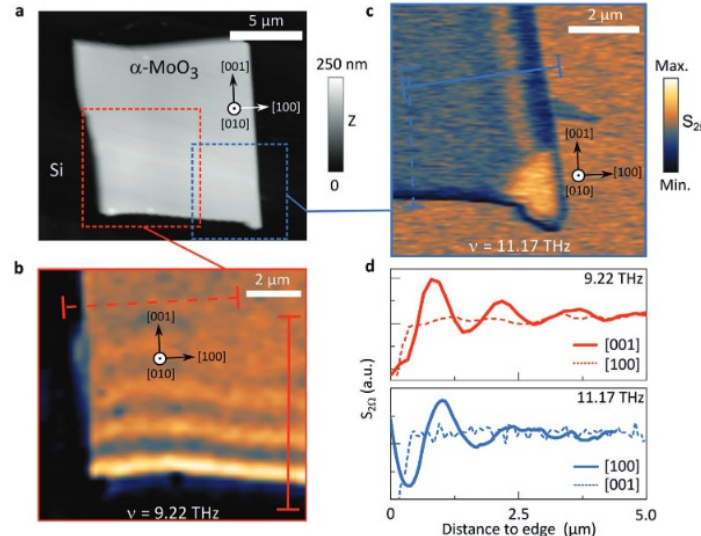
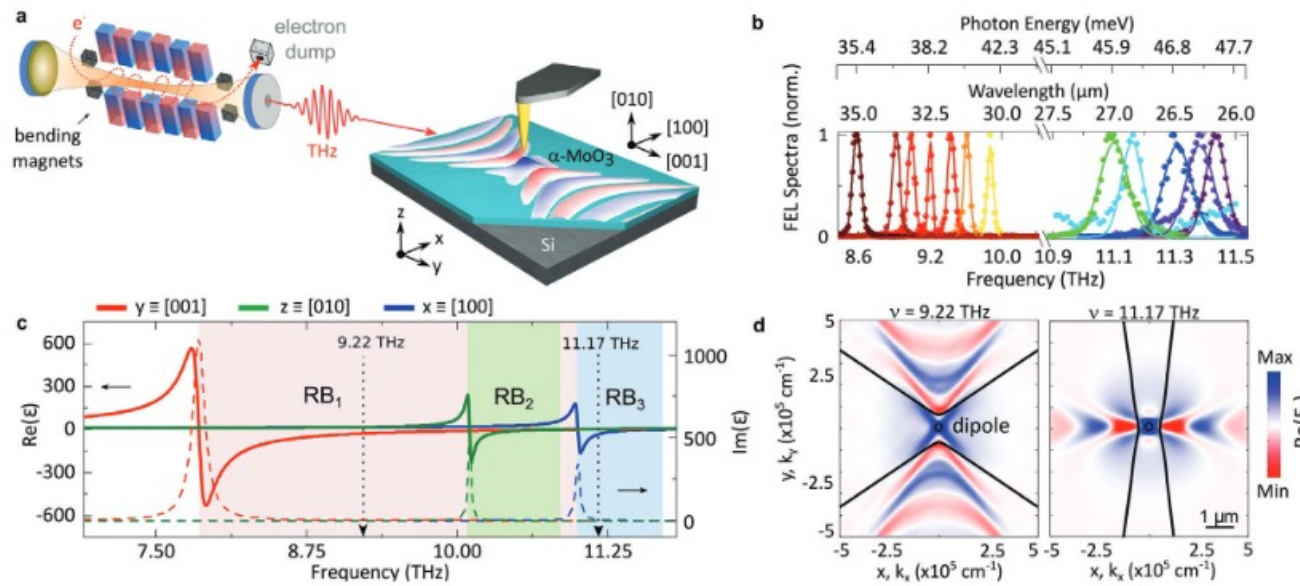
Narrowband THz

Cavity FEL *FELBE*



Nanoscale THz phonon polaritons

FELBE



Near-field images show periodic signals (fringes) parallel to specific flake edges. This reveals PhPs propagating with strongly in-plane anisotropic character.

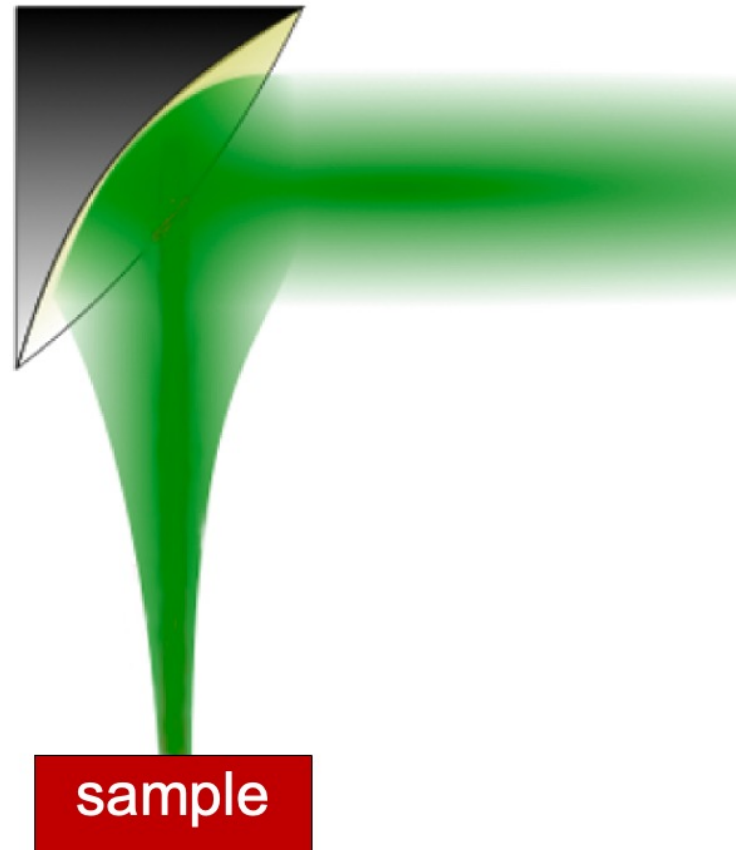
At 9.22 THz the polariton wavelength is $2.82 \mu\text{m} \ll \lambda_0 = 32.5 \mu\text{m}$

At 11.7 THz the polariton wavelength is $3.9 \mu\text{m} \ll \lambda_0 = 26.8 \mu\text{m}$



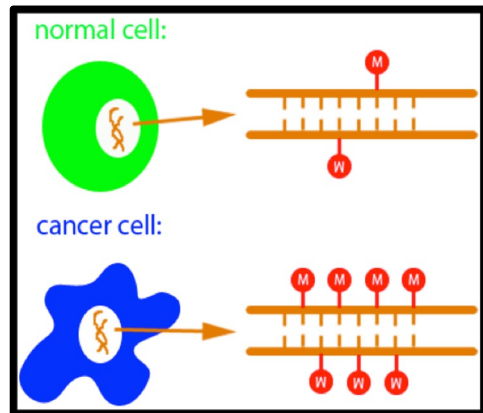
Elettra
Sincrotrone
Trieste

Terahertz Irradiation



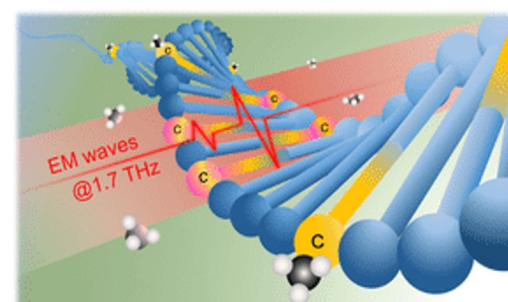
THz irradiation

THz-induced demethylation

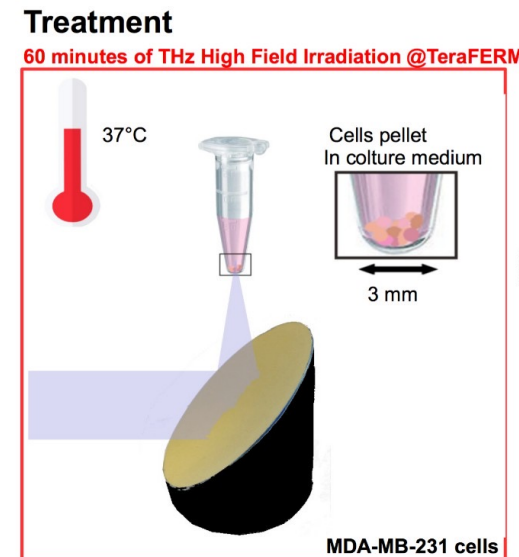


Cancer cells can show enhanced DNA Methylation

Methyl groups



Intense resonant THz radiation induces DNA demethylation



F. Piccirilli, M. Pachetti et al. (2021)

TeraFERMI

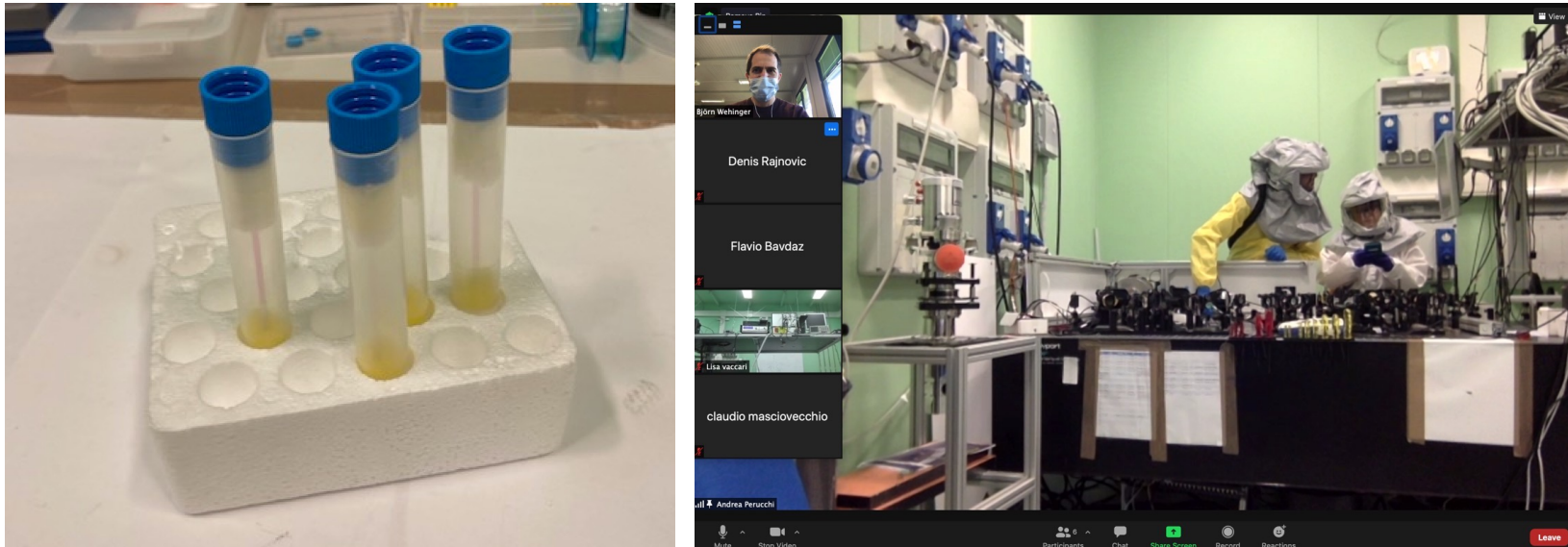
THz irradiation

Virus inactivation through THz irradiation

RNA modes resonate at THz frequencies

→ Inducing RNA damage while keeping the capsid intact

→ vaccines



Most plastics are transparent to THz radiation
Unbreakable sample holders can be used
Virus is sealed within 2 plastic containers



Elettra
Sincrotrone
Trieste

Acknowledgments

TeraFERMI

P. Di Pietro

J. Schmidt (*now @ Uni Nova Gorica*)

N. Adhlakha

Z. Ebrahimpour (*now at TIMEX*)

F. Piccirilli

SISSI-Bio

L. Vaccari

G. Birarda

F. Piccirilli

D. Bedolla

M.C. Stani

SISSI-MAT

S. Lupi

M. Zacchigna

V. Stopponi





Elettra
Sincrotrone
Trieste



A wide-angle aerial photograph of the Elettra Sincrotrone Trieste facility. The facility is a large complex of modern buildings, including a prominent circular building with a white roof and various industrial structures. It is situated in a green, hilly area with a road network. In the background, a coastal city with a harbor and mountains is visible under a clear blue sky.

THANK YOU

www.elettra.eu